

# UC Berkeley

## UC Berkeley Previously Published Works

### Title

The regulatory and transcriptional landscape associated with carbon utilization in a filamentous fungus

### Permalink

<https://escholarship.org/uc/item/45q8249t>

### Journal

Proceedings of the National Academy of Sciences of the United States of America, 117(11)

### ISSN

0027-8424

### Authors

Wu, Vincent W  
Thieme, Nils  
Huberman, Lori B  
[et al.](#)

### Publication Date

2020-03-17

### DOI

10.1073/pnas.1915611117

### Supplemental Material

<https://escholarship.org/uc/item/45q8249t#supplemental>

Peer reviewed

1 **The regulatory and transcriptional landscape associated with carbon**  
2 **utilization in a filamentous fungus**

3  
4 Vincent W. Wu<sup>a,b</sup>, Nils Thieme<sup>c,g</sup>, Lori B. Huberman<sup>a,b</sup>, Axel Dietschmann<sup>c,f</sup>, David J.  
5 Kowbel<sup>a</sup>, Juna Lee<sup>d</sup>, Sara Calhoun<sup>d</sup>, Vasanth Singan<sup>d</sup>, Anna Lipzen<sup>d</sup>, Yi Xiong<sup>a,b,h</sup>,  
6 Remo Monti<sup>d</sup>, Matthew J. Blow<sup>d</sup>, Ronan C. O'Malley<sup>d</sup>, Igor V. Grigoriev<sup>d,5</sup>, J. Philipp  
7 Benz<sup>d</sup>, N. Louise Glass<sup>a,b,e,1</sup>

8  
9 <sup>a</sup>Department of Plant and Microbial Biology, University of California, Berkeley,

10 <sup>b</sup>Energy Biosciences Institute, University of California, Berkeley,

11 <sup>c</sup>Holzforchung München, TUM School of Life Sciences Weihenstephan, Technical  
12 University of Munich, Freising, Germany, <sup>d</sup>Joint Genome Institute, Walnut  
13 Creek, CA

14 <sup>e</sup>Environmental Genomics and Systems Biology, Lawrence Berkeley National  
15 Laboratory, Berkeley, CA

16 <sup>f</sup>current address: Chair of Microbiology, TUM School of Life Sciences Weihenstephan,  
17 Technical University of Munich, Freising, Germany

18 <sup>g</sup>current address: Department of Infection Biology, Institute for Clinical Microbiology,  
19 Immunology and Hygiene, Universitätsklinikum Erlangen and Friedrich-  
20 Alexander Universität, Erlangen-Nürnberg, Germany

21 <sup>h</sup>current Address: Amyris, Inc. Emeryville, CA

22  
23 <sup>1</sup>Corresponding Author: N. Louise Glass

24 [Lglass@berkeley.edu](mailto:Lglass@berkeley.edu)

25  
26 Keywords: Regulatory networks, nutrient signaling, plant biomass, cellulases,  
27 pectinases, hemicellulases, DAP-seq, Neurospora, major facilitator transporters,  
28 carbon catabolite repression

29  
30 Classification: Biological Sciences, Genetics

31

## 32 **Abstract**

33 Filamentous fungi, such as *Neurospora crassa*, are very efficient in deconstructing  
34 plant biomass, ~~both by the secretion of~~ an arsenal of plant cell wall  
35 degrading enzymes, ~~and~~ by remodeling metabolism to accommodate production of  
36 secreted enzymes and ~~by~~ enabling transport and intracellular utilization of plant  
37 biomass components. Although a number of enzymes and transcriptional regulators  
38 involved in plant biomass utilization have been identified, how filamentous fungi  
39 sense and integrate nutritional information encoded in the plant cell wall into a  
40 regulatory hierarchy for optimal utilization of complex carbon sources is not  
41 understood. Here we performed transcriptional profiling of *N. crassa* on 40 different  
42 carbon sources, including plant biomass, to provide data on how fungi sense simple  
43 to complex carbohydrates. From these data, we identified new regulatory factors in  
44 *N. crassa* and characterized one (PDR-2) associated with pectin utilization one with  
45 pectin/hemicellulose utilization (ARA-1). Using *in vitro* DNA-affinity purification  
46 sequencing (DAP-seq), we identified direct targets of transcription factors involved  
47 in regulating ~~genes encoding plant cell wall degrading enzyme~~  
48 ~~genes~~. In particular, our data clarified the role of the transcription factor VIB-1 in the  
49 regulation of genes encoding PCWDEs and nutrient scavenging and revealed a  
50 major role of the carbon catabolite repressor CRE-1 in regulating the expression of  
51 major facilitator transporter genes. These data contribute to a more complete  
52 understanding of crosstalk between transcription factors and their target genes,  
53 which are involved in regulating nutrient sensing and plant biomass utilization on a  
54 global level.

55

## 56 **Significance statement**

57 Microorganisms have evolved signaling networks to identify and prioritize utilization  
58 of carbon sources. For fungi that degrade plant biomass, such as *Neurospora*  
59 *crassa*, signaling networks dictate the metabolic response to carbon sources  
60 present in plant cell walls, resulting in optimal utilization of nutrient sources.  
61 However, within a fungal colony, regulatory hierarchies associated with activation of  
62 transcription factors and temporal and spatial production of proteins for plant  
63 biomass utilization are unclear. Here, we perform expression profiling of *N. crassa*  
64 on simple sugars to complex carbohydrates to identify regulatory factors and direct  
65 target of regulatory transcription factors using DNA-affinity purification sequencing

66 (DAP-seq). These findings will enable more precise tailoring of metabolic networks  
67 in filamentous fungi for the production of second-generation biofuels.  
68

## 69 **Introduction**

70 In nature, fungi must integrate acquisition of nutrients with metabolism,  
71 growth and reproduction. Fungal deconstruction of plant biomass by fungi requires  
72 the ability to efficiently produce and secrete large quantities of secreted plant cell  
73 wall degrading enzymes (PCWDEs). Turnover of plant biomass by fungi is an  
74 ecosystem function (1), as well as an attribute that has been harnessed industrially  
75 to convert plant biomass to simple sugars and in turn high value compounds (2).  
76 The plant cell wall is composed of a complex and integrated set of polysaccharides  
77 that can vary across tissue type and plant species. Cellulose is the most recalcitrant  
78 and most abundant cell wall polysaccharide and is composed of  $\beta$ -1,4-linked D-  
79 glucose residues arranged in linear chains. Hemicelluloses represent about 20-35%  
80 of primary plant cell wall biomass, and include polysaccharides with  $\beta$ -1,4-linked  
81 backbones, such as xylan, xyloglucan and mannan. Pectin is a heterogeneous  
82 structure with an abundance of D-galacturonic acid, L-rhamnose and L-arabinose.  
83 The two most common forms of pectin are homogalacturonan, which is composed of  
84 a D-galacturonic acid backbone, and rhamnogalacturonan I, which has a backbone  
85 consisting of alternating galacturonic acid and rhamnose residues. Both forms have  
86 a diverse array of side-chains (3). Pectins are crosslinked with hemicellulose and  
87 cellulose and affect plant cell wall pore size, flexibility and strength. Lignin, which  
88 adds rigidity to the plant cell wall, is composed of polymers of aromatic residues  
89 and is very recalcitrant to deconstruction (4).

90 Although biochemical activities of select PCWDEs have been investigated in a  
91 variety of filamentous fungi, how fungi sense complex carbohydrates in plant  
92 biomass, and how that sensing is transduced intracellularly into a hierarchical  
93 metabolic response resulting in optimal production of PCWDEs and integration of  
94 cellular metabolism is unclear. The production of PCWDEs is dependent on  
95 transcription factors that modulate expression of these genes upon appropriate  
96 nutrient sensing. In *Neurospora crassa*, *Aspergillus nidulans*, *Aspergillus oryzae* and  
97 *Penicillium oxalicum*, the transcription factor CLR-2 (ClrB/ManR) is the major  
98 regulator of genes involved in the deconstruction of cellulose (5, 6), while in  
99 *Trichoderma reesei* and *Aspergillus niger*, the transcription factor Xyr1/XlnR  
100 regulates genes involved in both cellulose and hemicellulose degradation (7, 8). In  
101 species like *N. crassa* and *Fusarium graminearum*, XlnR homologs regulate genes  
102 involved in hemicellulose utilization (9, 10). Transcription factors associated with

103 pectin deconstruction include RhaR/PDR-1, GaaR and, Ara1. In *A. niger* and *N.*  
104 *crassa*, RhaR/PDR-1 are required for rhamnose utilization (11, 12), while in *B.*  
105 *cinerea* and *A. niger*, GaaR is responsible for galacturonic acid utilization (13, 14). In  
106 *A. niger*, the AraR transcription factor modulates arabinose utilization, while a  
107 different transcription factor (Ara1) functions in an analogous manner in  
108 *Magnaporthe oryzae* and *T. reesei* (15, 16). Additional transcriptional regulators that  
109 affect expression of genes encoding PCWDEs include the carbon catabolite  
110 repressor protein CreA/CRE-1 (17, 18), COL-26/BglR (19, 20) and VIB-1/Vib1 (21,  
111 22).

112         Here we performed transcriptional profiling of *N. crassa* on 40 different  
113 carbon sources to provide data on how fungi sense simple to complex  
114 carbohydrates and analyzed profiling data to identify regulatory factors associated  
115 with carbon source sensing and the regulation of transcriptional responses. From  
116 this approach, two transcription factors, one involved in pectin utilization, PDR-2  
117 and one involved in pectin and hemicellulose utilization, ARA-1, were identified and  
118 their regulons characterized. Using *in vitro* DNA-affinity purification sequencing  
119 (DAP-seq) of transcription factors involved in regulating PCWDE-encoding genes led  
120 to a more complete understanding of direct targets of these regulatory proteins and  
121 of the crosstalk between transcription factors involved in regulating nutrient sensing  
122 on a global level. In particular, our data clarified the role of VIB-1 in the regulation of  
123 genes encoding PCWDEs and nutrient scavenging and identified a previously  
124 overlooked mechanism of the carbon catabolite repressor protein CreA/CRE-1 in  
125 regulating cellular responses to carbon sources.

126

## 127 **Results**

### 128 ***N. crassa* carbon metabolism is distinctly regulated in response to** 129 **different carbon sources**

130         To improve our understanding of how regulatory networks are integrated  
131 during plant biomass utilization by filamentous fungi, we assessed gene expression  
132 patterns across 40 different carbon conditions in *N. crassa* (Table S1). To reduce the  
133 effects of differential growth on gene expression in different carbon sources, we  
134 performed switch experiments where *N. crassa* cells (FGSC2489) were pre-grown in  
135 sucrose as a sole carbon source (16 h), washed, and then transferred to media  
136 containing the experimental carbon source for 4 h prior to RNA extraction. The

137 carbon sources were divided into three categories: plant biomass, complex  
138 polysaccharides found in the plant cell wall, and the mono- and disaccharide  
139 building blocks that make up these complex polysaccharides. We compiled a list of  
140 113 genes encoding predicted PCWDEs in the *N. crassa* genome (Table S2) and  
141 assessed expression of this gene set across our carbon panel (Fig. 1A; SI Dataset 1).

142 At low concentrations, various monosaccharides, disaccharides, and  
143 oligosaccharides induce the expression of genes encoding PCWDEs (23, 24). We  
144 exposed *N. crassa* to 19 different mono- and disaccharides at 2 mM concentration;  
145 this concentration of cellobiose was previously shown to induce robust expression of  
146 cellulolytic genes in *N. crassa* (23) (Table S1). As predicted, *N. crassa* induced genes  
147 encoding cellulases in response to cellobiose, genes encoding starch-degrading  
148 enzymes in response to maltose, genes encoding hemicellulases in response to  
149 xylose and arabinose, and genes encoding pectin deconstruction enzymes upon  
150 exposure to rhamnose and galacturonic acid (Fig. 1A; SI Dataset 1). However,  
151 individual sugars were also capable of inducing expression of PCWDEs not  
152 responsible for degrading their parent polymer. For example, cellobiose induced  
153 expression of some genes encoding some xylanases and pectinases in addition to  
154 cellulases, and arabinose induced expression of some genes encoding some  
155 cellulases in addition to arabinases (SI Dataset 1). These data indicate metabolic  
156 crosstalk between sugar sensing pathways and/or overlap in regulatory networks. *N.*  
157 *crassa* also showed strong transcriptional responses to complex plant biomass  
158 substrates, such as corn stover (a monocotyledonous plant of the grass family)  
159 ~~versus and~~ wingnut (*Pterocarya*; a hardwood tree from the walnut family) (Fig. 1A).

160 Mono-, di-, and oligosaccharides require transport into the cell for utilization  
161 and/or signaling for induction of genes encoding PCWDEs. Annotated sugar  
162 transporters belong to the Major Facilitator Superfamily (MFS) and led us to  
163 hypothesize that uncharacterized sugar transporters would also come from this  
164 protein family. To test this hypothesis, we constructed a maximum likelihood tree  
165 using protein sequences from all MFS transporters in the *N. crassa* genome (Fig.  
166 S1). The majority of predicted sugar transporters with the exception of NCU05897  
167 (fucose permease) and NCU12154 (maltose permease), fell into a single  
168 monophyletic clade corresponding to family 2.A.1.1 of the transporter classification  
169 database (TCDB; (25)). Of the predicted sugar transporters in this clade, five un-  
170 annotated MFS transporters (NCU04537, NCU05350, NCU05585, NCU06384,

171 NCU07607) had increased expression on unique sugars and complex carbon  
172 sources, suggesting potential involvement in catabolism of those carbon sources  
173 (Fig. S1; Dataset S1).

174 To evaluate crosstalk between regulatory pathways that coordinate  
175 expression of PCWDEs, we performed weighted gene co-expression network  
176 analysis (WGCNA) (26) across the transcriptional dataset and identified twenty-eight  
177 modules of co-expressed genes (Fig. 1B; SI Dataset 2) that showed enrichment of  
178 specific functional classifications (Fig. S2). The majority of PCWDE genes were found  
179 within three modules. Module 1 (red; n= 153) contained gene encoding PCWDEs  
180 that are upregulated in response to cellulose and hemicellulose along with notable  
181 transcription factors *xlr-1*, *clr-1*, *clr-2*, *hac-1*, and *vib-1* (21, 27, 28). This module also  
182 contained 55 genes that encoded hypothetical proteins. Module 2 (yellow; n=42)  
183 contained the majority of predicted pectin metabolic genes (28) and eight genes  
184 encoding hypothetical proteins. Module 3 (blue; n=42) contained a number of  
185 predicted pentose catabolic genes along with some notable xylanases and xylose  
186 transporters and nine genes encoding hypothetical proteins (SI Dataset 2; Fig. S2).  
187 An additional module (Module 4; n=142; midnight blue) clustered closely with  
188 modules 1 and 3. This module was significantly enriched for genes encoding ER and  
189 protein processing proteins (cellular transport and protein fate; Fig. S2) that are co-  
190 regulated with genes encoding cellulases and xylanases, such as various COPII  
191 proteins, SEC-61, KEX2, (SI Dataset 1; SI Dataset 2). This module also included  
192 genes encoding 29 hypothetical proteins.

193

### 194 **Defining the PCWDE transcriptional network**

195 Prior studies in *N. crassa* identified conserved transcription factors that are  
196 positive regulators of cellulase and some hemicellulase genes (CLR-1/CLR-2),  
197 xylanase and xylose utilization genes (XLR-1), pectin-degrading genes (PDR-1), and  
198 starch catabolic genes (COL-26) (10, 11, 19, 27). We hypothesized that it would be  
199 possible to identify additional regulators involved in plant cell wall degradation by  
200 looking for transcription factors with a similar expression profile to a specific class of  
201 genes encoding PCWDEs using hierarchical clustering. A systematic analysis of  
202 expression profiles of 336 proteins with predicted DNA-binding domains identified  
203 34 additional transcription factors that were specifically induced on different plant  
204 biomass components (Table S3A). We hypothesized that strains carrying a deletion



205 of a transcription factor would display an altered transcriptional profile under the  
206 conditions where they were most highly expressed (Table S3B). When the  
207 corresponding deletion strains were tested under the respective induction  
208 conditions, a majority of the 34 transcription factor deletion mutants did not display  
209 a clear expression phenotype as compared to the parental strain, FGSC2489.  
210 However, deletion mutants for two transcription factors showed a consistent and  
211 obvious role in PCWDE expression, NCU04295 and NCU05414 (SI Dataset 3).

212 The expression of NCU04295 clustered with genes encoding pectin-degrading  
213 enzymes (SI Dataset 3) and a  $\Delta$ NCU04295 mutant showed decreased expression  
214 levels of genes necessary for pectin utilization when grown in presence of pectin-  
215 rich citrus peel as compared to wild type cells on citrus peel (Fig. 2A, B; SI Dataset  
216 3). The genes with the largest decrease in expression level in  $\Delta$ NCU04295 as  
217 compared to wild type included pectate lyases genes *ply-1* and *ply-2* (NCU06326  
218 and NCU08176), the galacturonic acid transporter gene *gat-1* (NCU00988), the exo-  
219 polygalacturonase genes *gh28-2* (NCU06961), and orthologs of *gaaA*, *gaaB* and  
220 *gaaC* (NCU09533, NCU07064 and NCU09532), encoding enzymes for galacturonic  
221 acid catabolism (Fig. 2B; SI Dataset 3). The predicted protein sequence of  
222 NCU04295 showed similarity (~50% amino acid identity) to GaaR, which plays a  
223 role in galacturonic acid metabolism in *B. cinerea* and *A. niger* (13, 14). We  
224 therefore named NCU04295 *pdr-2* for pectin degradation regulator-2. Consistent  
225 with its predicted function, the  $\Delta$ *pdr-2* mutant showed a severe growth defect in  
226 medium containing pectin or galacturonic acid as the sole carbon source and  
227 significantly reduced pectate lyase and endo-polygalacturonanase activity (Fig.  
228 2C,D). A second pectin degradation regulator previously identified in *N. crassa*, *pdr-1*,  
229 also shows a severe growth defect on pectin (11). However, unlike  $\Delta$ *pdr-1* cells,  
230  $\Delta$ *pdr-2* cells grew on L-rhamnose as the sole carbon source (Fig. S3), suggesting  
231 distinct roles for PDR-2 and PDR-1 in regulating pectin degradation. A strain bearing  
232 both *pdr-1* and *pdr-2* deletions mimicked the phenotype of either a  $\Delta$ *pdr-1* or a  
233  $\Delta$ *pdr-2* mutant (Fig. 2C, D), but did not cause a complete abolition of growth with  
234 pectin as the sole carbon source (Fig. S3).

235 NCU05414 displayed high expression on *Miscanthus* biomass (SI Dataset 1).  
236 When compared to wild type cells exposed to 1% *Miscanthus*, a  $\Delta$ NCU05414 mutant  
237 showed reduced expression of genes encoding several arabinosidases (NCU09924,  
238 NCU9775), two  $\beta$ -xylosidases (NCU00709, NCU09923), the L-arabinose transporter

239 *lat-1* (NCU02188), and L-arabinitol dehydrogenase *ard-1* (NCU00643) (Fig. 2E; SI  
240 Dataset 3), suggesting that the  $\Delta$ NCU05414 mutant would be defective for  
241 utilization of arabinan, arabinose and galactose. As predicted, the  $\Delta$ NCU05414  
242 strain showed dramatically reduced growth on 2% arabinan, arabinose, and  
243 galactose, but was able to metabolize hemicellulose and pectin substrates (Fig. 2F).  
244 When NCU05414 was placed under the regulation of the strong constitutive  
245 promoter *gpd-1* (oxNCU05414), cells showed increased growth on arabinose relative  
246 to wild type (Fig. S3) and increased expression of *ard-1* (LADH; Fig. 2G), further  
247 supporting positive regulation of arabinose metabolic genes by NCU05414. The  
248 NCU05414 predicted protein showed significant similarity to the Ara1 protein in *T.*  
249 *reesei* and *Magnaporthe oryzae*, where it plays a role in arabinose metabolism and  
250 arabinose and galactose catabolism, respectively (16, 29). We therefore named  
251 NCU05414 *ara-1*.

252 Many PCWDEs involved in degradation of heterogeneous substrates like  
253 pectin and hemicellulose are under the control of multiple transcription factors. We  
254 constructed regulons of transcription factors important for plant biomass  
255 deconstruction based on the genes that are differentially expressed between  
256 transcription factor mutant versus wild-type cells (*clr-1*, *clr-2*, *xlr-1*, *pdr-2*, *ara-1*; SI  
257 Dataset 3) and from previous studies for *col-26* and *pdr-1* (11, 19). The regulons of  
258 CLR-1, CLR-2, XLR-1, PDR-1, PDR-2, ARA-1 and COL-26 showed extensive overlap  
259 (Fig. 3). As an example, the expression of the putative acetylxylan esterase gene  
260 (*ce1-1* NCU04870), an enzyme responsible for cleaving acetyl groups from xylan  
261 and critically important for increasing accessibility of xylan to xylanases, relative to  
262 wild type cells showed a 20-fold decrease in expression levels in  $\Delta$ *clr-2* cells after a  
263 shift to Avicel, a 500-fold decrease in expression in  $\Delta$ *xlr-1* cells after a shift to xylan,  
264 and a 7-fold decrease in expression in  $\Delta$ *pdr-2* cells after a shift to citrus peel (SI  
265 Dataset 3). Moreover, the *ce1-1* promoter was shown to be directly bound by both  
266 XLR-1 and CLR-2 by chromatin-immunoprecipitation-sequencing (ChIP-seq) (10).

267

## 268 **Utilizing DAP-seq to identify direct targets of *N. crassa* transcription** 269 **factors.**

270 The transcriptional regulons associated with plant biomass deconstruction  
271 identified above could be due to direct or indirect regulation of target genes by a  
272 particular transcription factor. To define the direct regulons of transcription factors

273 involved in plant biomass deconstruction, we used DAP-seq, where *in vitro*  
274 synthesized transcription factors are used for affinity purification of bound  
275 sequences in sheared genomic DNA, which are subsequently identified via DNA  
276 sequence analyses (30). To ensure that DAP-seq was an effective method for  
277 identifying direct binding sites of transcription factors involved in plant cell wall  
278 deconstruction in *N. crassa*, we confirmed the DNA binding sites of CLR-1 and XLR-  
279 1, for which ChIP-seq data are available (10).

280 We re-analyzed promoter regions of genes (defined as within 3 kb of the ATG  
281 start site) bound by XLR-1 identified via ChIP-seq (10) (SI Dataset 4) and bound  
282 promoter regions identified via DAP-seq data where transcription was reduced by at  
283 least 2<sup>1.5</sup> (2.8)-fold via differential RNA-seq analysis of WT versus an  $\Delta xlr-1$  mutant  
284 (SI Datasets 3 and 4). We identified 85 XLR-1 target genes using ChIP-seq data and  
285 78 genes via DAP-seq, with 47 genes shared between the two datasets (Fig.  
286 S4A,C,F; SI Dataset 4). The binding site sequences from the 78 genes identified in  
287 the DAP-seq dataset were used to build an XLR-1 consensus binding motif, which  
288 was comparable to the one reported from ChIP-seq data analysis (10) (Fig. S4G).  
289 Using the same methods to explore CLR-2, we identified 87 genes with CLR-2-bound  
290 promoters via DAP-seq and 65 genes with CLR-2-bound promoters via ChIP-seq; 48  
291 genes were shared between datasets (Fig. S4D, E, F; SI Dataset 3 and 4). Slight  
292 differences were identified in the CLR-2 consensus binding sequence using DAP-seq  
293 versus that previously reported for ChIP-seq data (10) (Fig. S4G).

294 Neither the ChIP-seq nor DAP-seq method reliably reduced ~~false positives,~~  
295 ~~which we defined as the number of~~ genes whose promoters were bound by the  
296 transcription factor, but whose transcription was not differentially expressed  
297 between wild type and the transcription factor mutant under the conditions tested.  
298 For example, the CLR-2 ChIP-seq identified 158 genes with promoter regions  
299 bound, while DAP-seq identified 1683; however, the majority of DAP-seq bound  
300 genes were not differentially expressed in a  $\Delta clr-2$  mutant relative to WT cells. For  
301 XLR-1, ChIP-seq identified 1117 genes, while DAP-seq identified 531 (SI Dataset 4).  
302 Thus, ~~only through a~~ comparison ~~of with RNA-seq data and~~ differential expression  
303 analyses between WT and transcription factor mutants ~~helped to filter~~ could the  
304 ChIP-seq and DAP-seq datasets ~~be filtered~~ for biologically relevant genes for these  
305 specific transcription factors. For the remaining genes whose expression was not  
306 altered in the TF mutants, it is unclear whether they are “false positive” or genes

307 [that might be regulated by CLR-2 or XLR-1 under different conditions that were not](#)  
308 [assessed in this study.](#)

309 In *T. reesei*, a constitutively active *xyr1* allele (ortholog to *N. crassa xlr-1*)  
310 contains a single amino acid substitution (alanine to valine) in the C-terminal  
311 predicted alpha helix (31). The construction of the orthologous mutation (A828V) in  
312 *N. crassa xlr-1* results in a strain that shows inducer-independent expression and  
313 production of hemicellulases (10). To test whether this mutation affected the  
314 binding affinity of XLR-1, we also performed DAP-seq on the XLR-1<sup>A828V</sup> mutant. The  
315 binding targets of the XLR-1<sup>A828V</sup> mutant largely overlapped with the binding targets  
316 of XLR-1, indicating that the A828V mutation has little or no influence on XLR-1 DNA  
317 binding affinity (Fig. S4B,F; SI Dataset 4).

318

### 319 **DAP-seq suggests a multi-tiered system of CRE-1-mediated carbon** 320 **catabolite repression**

321 CRE-1 is a major regulator of carbon catabolite repression (CCR), a process  
322 through which the expression of genes involved in the utilization of non-preferred  
323 carbon sources is repressed in the presence of preferred carbon sources (32).  
324 Although many PCWDEs are known to be regulated by carbon catabolite repression,  
325 it was unclear whether this repression was directly or indirectly mediated by CRE-1.  
326 Using DAP-seq, we identified 329 CRE-1 binding sites in 318 promoter regions, with  
327 11 promoters showing two peaks (SI Dataset 4). The 318 genes with promoters  
328 bound by CRE-1 were enriched for 30 functional categories (p-value < 1x10<sup>-5</sup>)  
329 [involved in metabolic and catabolic activities](#) (Table S4). The top 17 functional  
330 categories were all involved in carbon metabolism, specifically cellulose,  
331 hemicellulose, pectin, and starch catabolism, representing approximately 50% of  
332 the total CRE-1 peaks [and consistent with functions associated with CRE-1](#). We used  
333 the sequences from CRE-1 bound peaks to build a consensus core motif with the  
334 best fit core motif being 5'-TSYGGGG-3' (E=2.7x10<sup>-23</sup>), similar to the 5'-SYGGRG-3'  
335 motif described for CreA in *A. nidulans* (33) (Fig. S3C).

336 If CRE-1 directly represses genes encoding PCWDEs, we would expect to see  
337 CRE-1 binding of PCWDE promoter regions. However, only 19 of 113 PCWDE genes  
338 had CRE-1 binding sites in the promoter (SI Dataset 4). According to the “double-  
339 lock” mechanism proposed for Cre1 in *Aspergillus nidulans* (34), indirect repression  
340 of PCWDE expression by CRE-1 could either be due to CRE-1 repression of

341 transcription factors required for PCWDE gene activation or due to CRE-1 repression  
342 of genes necessary to activate those transcription factors. In our DAP-seq dataset,  
343 promoters for only two carbon transcription factors were bound by CRE-1, *clr-1* and  
344 *ara-1*. However, CRE-1 binding was highly biased for promoters of genes encoding  
345 MFS transporters (22 MFS genes), with 15 falling within the major sugar transporter  
346 clade (Fig. S1), including one high affinity glucose transporter, *hgt-1* NCU10021 (35)  
347 and additional uncharacterized transporters (NCU00809, NCU06522, NCU09287,  
348 NCU04537, NCU01494, NCU06384, and NCU05897).

349 CRE-1 also bound to the promoters of the cellodextrin transporters *cdt-1*  
350 (NCU00801), *cdt-2* (NCU08114), and *sut-12/cbt-1* (NCU05853) (36-39). Cells lacking  
351 both *cdt-1* and *cdt-2* are unable to activate cellulolytic gene transcription and do not  
352 grow on cellulose (40). The binding of CRE-1 to the promoter of *clr-1* likely  
353 contributes to the repression of cellulolytic genes by CRE-1, as CLR-1 positively  
354 regulates *clr-2*, the major regulator of cellulolytic genes in *N. crassa* (10, 27)(Fig. 4;  
355 SI Dataset 4). ~~CRE-1 also bound to the promoters of the cellodextrin transporters-~~  
356 ~~*cdt-1* (NCU00801), *cdt-2* (NCU08114), and *sut-12/cbt-1* (NCU05853) (36-39). Cells~~  
357 ~~lacking both *cdt-1* and *cdt-2* are unable to activate cellulolytic gene transcription~~  
358 ~~and do not grow on cellulose (40).~~ Our data therefore suggested that cellulolytic  
359 gene expression is repressed by CRE-1 through a combination of direct binding to  
360 cellodextrin transporters, the transcription factor *clr-1* and a few cellulolytic  
361 PCWDEs, the transcription factor *clr-1*, and cellodextrin transporters (Fig. 4).

362 For genes involved in hemicellulose deconstruction, CRE-1 binding sites were  
363 detected in the promoters of the arabinose-transporter *lat-1* (NCU02188) (28),  
364 xylose transporters NCU00821 and NCU04527 (41), the xylodextrin transporter *cdt-*  
365 2, which is required for wild type-levels of growth on xylan (38), and pentose  
366 transporters *xat-1* (NCU01132) and *xyt-1* (NCU05627) (42) (Fig. 4). CRE-1 binding  
367 peaks were not detected in the promoter of the major transcriptional regulator of  
368 xylan utilization, *xlr-1*, although CRE-1 binding sites were detected in the promoter  
369 of the arabinose utilization regulator, *ara-1*; an  $\Delta$ *ara-1* mutant showed dramatically  
370 reduced growth on arabinan, arabinose, and galactose (Fig. 2). CRE-1 also directly  
371 bound to promoters of genes encoding xylanases, galactosidases, and  
372 arabinanases, as well as genes necessary for arabinose metabolism (SI Dataset 4)-  
373 ~~CRE-1 binding peaks were not detected in the promoter of the major transcriptional~~  
374 ~~regulator of xylan utilization, *xlr-1*. However, CRE-1 binding sites were detected in-~~

375 ~~the promoter of the arabinose utilization regulator, *ara-1*; an  $\Delta$ *ara-1* mutant showed~~  
376 ~~dramatically reduced growth on arabinan, arabinose, and galactose (Fig. 2). CRE-1~~  
377 ~~binding sites were also detected in the promoter of the arabinose transporter *lat-1*~~  
378 ~~(NCU02188) (28), xylose transporters NCU00821 and NCU04527 (41), the~~  
379 ~~xylohextrin transporter *cdt-2*, which is required for wild type levels of growth on~~  
380 ~~xylan (38), and pentose transporters *xat-1* (NCU01132) and *xyt-1* (NCU05627) (42)~~  
381 ~~(Fig. 4).~~

382 CRE-1 was not bound to the *pdr-1* or *pdr-2* promoters, which are responsible  
383 for regulating the majority of pectinase genes in *N. crassa* (12; Fig. 2A). For genes  
384 involved in pectin utilization, DAP-seq showed However, CRE-1 binding sites were  
385 identified in the promoter of a major exo-polygalacturonase (NCU06961; *gh28-2*) as  
386 well as predicted metabolic enzymes for galacturonic acid utilization (*gaaA* ortholog  
387 NCU09533, *gaaB* ortholog NCU07064 and *gaaC* ortholog NCU09532) (Fig. 4; SI  
388 Dataset 4). ~~CRE-1 was not bound to the *pdr-1* or *pdr-2* promoters, which are~~  
389 ~~responsible for regulating the majority of pectinase genes. One of the~~  
390 uncharacterized sugar transporters bound by CRE-1, *sut-28* (NCU05897; annotated  
391 as a fucose permease; Fig. S1), is a predicted ortholog of the *A. niger* L-rhamnose  
392 transporter RhtA (43). The *sut-28* mutant showed reduced growth on L-rhamnose  
393 and, to a lesser extent, poly-galacturonic acid (Fig. 5A) and uptake of L-rhamnose in  
394 the  $\Delta$ *sut-28* cells was eliminated (Fig. 5B). Additionally, ~~s~~Similar to a  $\Delta$ *pdr-1* mutant,  
395  $\Delta$ *sut-28* cells failed to activate expression of the rhamnose catabolic gene L-  
396 rhamnonate dehydratase (NCU09034) (Fig. 5C). The expression of *sut-28* was  
397 higher in  $\Delta$ *cre-1* cells when exposed to L-rhamnose or L-rhamnose and glucose (Fig.  
398 S3D) and  $\Delta$ *cre-1* cells showed increased L-rhamnose uptake as compared to wild  
399 type when exposed to pectin and glucose (Fig. 5D). These data support the DAP-seq  
400 results indicating that CRE-1 negatively regulates the expression of *sut-28*. ~~Thus, an~~  
401 ~~important component of CRE-1 function includes the repression of transporter genes~~  
402 ~~that play a role in the uptake of signaling molecules acting as inducers of~~  
403 ~~transcription factors and genes associated with cellulose, hemicellulose and pectin-~~  
404 ~~utilization (Fig. 4).~~

405 A  $\Delta$ *cre-1* mutant shows growth defects relative to its wild-type parental strain  
406 when grown on sucrose (Sun and Glass 2011 PLoS One). Previous microarray data  
407 of a  $\Delta$ *cre-1* mutant relative to wild-type under minimal medium conditions with  
408 sucrose as the sole carbon source showed that 75 genes showed increased



409 expression levels (>2 fold) in the  $\Delta cre-1$  mutant (Sun and Glass 2011 PLoS One),  
410 seven of which encoded predicted MFS transporters. Of these 75 genes, the  
411 promoters of 21 genes were bound by CRE-1 in the DAP-seq dataset, a significant  
412 enrichment over random (3.5 genes), and which included all seven of the predicted  
413 MFS transporters that showed increased expression in the  $\Delta cre-1$  mutant relative to  
414 wild type. These MFS sugar transporters included NCU04537 (monosaccharide  
415 transporter), NCU04963 (high affinity glucose transporter), NCU06026 (quininate  
416 permease), NCU05897 (*sut-28*), NCU10021 (*hgt-1*), NCU00821 (sugar transporter)  
417 and NCU05627 (high affinity glucose transporter *hgt-1*). The remaining set of 21  
418 genes include a number of carbon metabolic enzymes and 5 genes encoding  
419 proteins of unknown function (SI Dataset 4). Thus, an important component of CRE-  
420 1 function includes the repression of transporter genes that play a role in the  
421 uptake of signaling molecules acting as inducers of transcription factors and genes  
422 associated with cellulose, hemicellulose and pectin utilization (Fig. 4).

423 ~~Thus, an important component of CRE-1 function includes the repression of~~  
424 ~~transporter genes that play a role in the uptake of signaling molecules acting as~~  
425 ~~inducers of transcription factors and genes associated with cellulose, hemicellulose-~~  
426 ~~and pectin utilization (Fig. 4).~~

427

428

## 429 **DAP-seq of VIB-1 reveals a global role in regulating carbon metabolism**

430 VIB-1 is a Zn<sub>2</sub>Cys<sub>6</sub> transcription factor first identified for its role in mediating  
431 self/nonself recognition and heterokaryon incompatibility in *N. crassa* (44, 45). The  
432  $\Delta vib-1$  mutant also shows severely reduced growth on Avicel and a weak induction  
433 of *clr-2* (21), a phenotype also observed in *T. reesei*  $\Delta vib1$  strains (22). In addition to  
434 Avicel, the  $\Delta vib-1$  mutant also has a severe growth defect on pectin and a moderate  
435 growth defect on xylan (Fig. S5A).

436 RNA-seq was previously performed on  $\Delta vib-1$  cells exposed to Avicel and  
437 carbon starvation conditions (21). Here, we performed additional RNA-seq  
438 experiments on the  $\Delta vib-1$  mutant exposed to 1% pectin or 1% xylan as the sole  
439 carbon source, 1% BSA as the sole carbon and nitrogen source, and 1% ground  
440 *Miscanthus* as the complete nutrient source (SI Dataset 5). RNA-seq data reflected  
441 the severity of growth phenotypes, as exposure to Avicel, pectin, and BSA displayed  
442 the greatest number of differentially expressed genes between WT and the  $\Delta vib-1$

443 mutant. Consistent with its phenotype, the  $\Delta vib-1$  mutant has a more similar  
444 expression profile to WT cells under xylan conditions.

445           Using DAP-seq, we identified VIB-1 binding sites within 1.5 kb  
446 upstream of the ATG start site of 1,742 genes (SI Dataset 4). The RNA-seq  
447 datasets were utilized to eliminate false positives from DAP-seq data by  
448 limiting the set to genes with at least a  $2^{1.5}$  (2.8)-fold change in gene  
449 expression in any of our six conditions. In total, we identified 238 direct  
450 target genes of VIB-1 (SI Dataset 5). Hierarchical clustering of gene  
451 expression data of these direct targets showed that one cluster included the  
452 majority of genes that were down regulated in the  $\Delta vib-1$  mutant in more  
453 than three conditions. We considered these genes to be the core regulon of  
454 VIB-1 (Fig. 6A). A consensus binding motif from VIB-1 peaks within the 1.5 kb  
455 promoter regions of core regulon genes showed conservation of three critical  
456 bases: T, A and C (Fig. 6CB).

457           The 56 gene VIB-1 core regulon included genes involved in  
458 heterokaryon incompatibility (*tol*, *pin-c* and *het-6*) and a number of  
459 uncharacterized genes encoding proteins with predicted roles in  
460 heterokaryon incompatibility (HET domain proteins and genes with  
461 polymorphic alleles in wild populations; NCU03533, NCU05840, NCU07335  
462 and NCU04453) (SI Dataset 5) (46). Most of the other annotated genes in the  
463 VIB-1 core regulon were associated with metabolism, including three  
464 arabinofuranosidases (NCU09170 NCU09975 and NCU02343), a beta-  
465 xylosidase (NCU09923), three cellulose PMOs (NCU02240, NCU09764 and  
466 NCU02344), a starch active PMO (NCU08746), a galacturonic acid  
467 transporter (*gat-1*; NCU00988), an exogalacturonase (NCU06961),  
468 rhamnogalacturonan acetyltransferase (NCU09976), a secreted phospholipase  
469 (NCU06650), and acid phosphatase (*pho-3*; NCU08643) (SI Dataset 5) (Fig.  
470 6B). Promoters of three genes encoding LaeA-like methyltransferase  
471 domains (NCU05841, NCU05832, and NCU05501) were in the core VIB-1  
472 regulon and four additional LaeA-like genes were direct targets of VIB-1  
473 (NCU04909, NCU04717, NCU04707, NCU01148) (SI Dataset 5). LaeA is a  
474 regulator of secondary metabolism in ascomycete fungi first described in *A.*  
475 *nidulans* (47).



476 The *clr-2* and *pdr-2* genes were the only ones encoding transcription factors  
477 that were direct targets of VIB-1 (Fig. 6B). In the  $\Delta vib-1$  mutant, expression of *clr-2*  
478 was reduced 5.2-fold relative to wild type during exposure to Avicel and expression  
479 of *pdr-2* was reduced 3.4-fold relative to wild type during exposure to pectin. In  
480 addition to *clr-2* and *pdr-2*, a number of PCWDE-encoding genes were bound and  
481 regulated by VIB-1, including genes encoding enzymes in the core VIB-1 regulon  
482 (above), cellulases (*gh6-3*, NCU07190; *gh45-1*, NCU05121, NCU05751),  
483 arabinosidase (NCU05965), rhamnogalacturonase (NCU05598),  
484 rhamnogalacturonan acetylerase (NCU09976), a pectinesterase (NCU10045),  
485 xylanases (NCU02855, NCU04997), feruloyl esterase B (NCU09491), and acetyl  
486 xylan esterases (NCU08785, NCU04494) (Fig. 6C). Additional genes encoding  
487 PCWDEs that were down-regulated in the  $\Delta vib-1$  mutant, but that did not have VIB-1  
488 binding sites in their promoters, could be explained by reduced expression of *clr-2*  
489 or *pdr-2* (Fig. 6C), consistent with the severe growth defect on cellulose and pectin  
490 substrates in the  $\Delta vib-1$  mutant.

491 Our DAP-seq data suggests that VIB-1 acts through *clr-2* to promote cellulase  
492 gene expression. However, ChIP-seq identified *vib-1* as a target of the cellulase  
493 regulator, CLR-1 (10). CLR-1 also binds to the promoter and is required for the  
494 expression of *clr-2* (10). These observations suggest an interplay in the regulation of  
495 *clr-2* by CLR-1 and VIB-1. To investigate these interactions, we measured cellulase  
496 production in a  $\Delta vib-1 \Delta clr-3$  strain, where repression of CLR-1 activation in the  
497 absence of cellulose is relieved (48) and in a  $\Delta vib-1 \Delta cre-1$  mutant, which eliminates  
498 regulation of *clr-1* by CRE-1. Both double mutant strains showed higher cellulase  
499 activity than  $\Delta vib-1$  cells (p-adj<0.01), indicating that when relieved from either  
500 CLR-3-or CRE-1-mediated repression, CLR-1 was capable of activating cellulolytic  
501 gene expression in the absence of VIB-1 (Fig. S5B). However, the cellulase activity  
502 of  $\Delta vib-1 \Delta clr-3$  or  $\Delta vib-1 \Delta cre-1$  cells was not as high as wild type cells, indicating  
503 that CLR-1 and VIB-1 were both required for full activation of cellulase genes in *N.*  
504 *crassa* (p-adj<0.01) (Fig. S5B).

505 In addition to defects in growth on cellulose and pectin, *N. crassa* and *A.*  
506 *nidulans vib-1/xprG* mutants show reduced growth when BSA is the sole carbon or  
507 nitrogen source (44, 49). However, analyses of the VIB-1 regulon on BSA did not  
508 reveal a clear reason for this growth deficit. Only three genes encoding predicted  
509 proteases/peptidases were significantly reduced in expression level in the  $\Delta vib-1$

510 mutant as compared to wild type cells, including a metalloprotease (*mpr-8*;  
511 NCU07200), a carboxypeptidase (*mpr-14*; NCU07536) and a proteinase T (*spr-7*;  
512 NCU07159). An additional set of vitamin B6 synthesis genes also showed decreased  
513 expression in the  $\Delta vib-1$  mutant specifically on BSA, including *pdx-1* (NCU06550)  
514 and *pdx-2* (NCU06549) that encode proteins that form the enzyme complex  
515 pyridoxal 5'-phosphate synthase or vitamin B6 synthase (SI Dataset 5). Pyridoxal  
516 5'-phosphate is a cofactor for many enzymes involved in amino acid metabolism  
517 and other protein metabolic processes (50).

518

## 519 **DISCUSSION**

520 In nature, the primary source of nutrients for *N. crassa* is plant biomass. In  
521 this study, we determined expression patterns of the laboratory strain of *N. crassa*  
522 to different types of carbon sources, including mono-, di-, oligosaccharides and  
523 plant biomass. These results showed that *N. crassa* responds specifically to the  
524 constituents of plant biomass in a largely specific manner (e.g. genes encoding  
525 cellulases were induced upon exposure of *N. crassa* to cellobiose), but also revealed  
526 cross regulation of genes encoding enzymes not found in the substrate (e.g. genes  
527 encoding some xylanases were induced upon exposure of *N. crassa* to cellobiose).  
528 Induction of PCWDEs by constituents of the plant cell wall, particularly cellobiose  
529 and xylose, have also been shown for other basidiomycete and ascomycete fungi  
530 (51-53). These data indicate that filamentous fungi respond specifically to the  
531 presence of the individual nutrient sources available, but also that the cells  
532 anticipate the presence of additional nutrient sources. This anticipation is likely due  
533 to the fact that individual components of the plant cell wall are unlikely to be found  
534 alone in nature and therefore expression profiles of fungi deconstructing plant  
535 biomass are shaped by the structure and composition of the plant cell wall.

536 Analyses of a large dataset of microarray transcriptomics data of *A. niger*  
537 exposed to different conditions and performed by multiple laboratories was used to  
538 generate co-expression networks (54). Here, WGCNA on *N. crassa* datasets from  
539 exposure to different carbon sources under carefully controlled conditions identified  
540 28 clusters of co-regulated genes (SI Dataset 2). We were particularly interested in  
541 defining new transcription factors and regulons associated with plant biomass  
542 deconstruction and identified 34 transcription factors whose expression level varied  
543 across our panel. Of these, two transcription factor mutants,  $\Delta ara-1$  and  $\Delta pdr-2$

544 showed a significantly different response to *Miscanthus* and pectin, respectively, as  
545 compared to WT cells (Fig. 2) and a deficiency in the utilization of  
546 arabinose/galactose ( $\Delta ara-1$ ) and galacturonic acid and pectin ( $\Delta pdr-2$ ). Our  
547 transcriptional analyses showed that the expression of the *lat-1* transporter gene  
548 and the *ard-1* gene were significantly down-regulated in the  $\Delta ara-1$  mutant. Loss of  
549 LAT-1 prevents arabinose transport (55), while *ard-1* encodes L-arabinitol-4-  
550 dehydrogenase, which catalyzes the second reaction of arabinose catabolism (56)  
551 as well as the third step of the oxidoreductive galactose catabolism (57). PDR-2 is  
552 involved in the regulation of genes encoding homogalacturonan backbone-  
553 degrading enzymes and galacturonic acid catabolic enzymes, similar to GaaR in *A.*  
554 *niger* and *B. cinerea* (13, 14). Activation of a number of pectinase genes, such as  
555 the endo-PGase *gh28-1*, were dependent on the presence of both PDR-1 and PDR-2  
556 (Fig. 2B,D). Further characterization of transcription factors associated with plant  
557 biomass deconstruction, including those identified in this study, will lead to a better  
558 understanding of metabolic crosstalk and reveal direct and/or indirect influence on  
559 each other in a synergistic regulatory network important for temporal and spatial  
560 deconstruction of plant biomass.

561 To define the direct regulons of transcription factors involved in plant  
562 biomass deconstruction, we utilized DAP-seq, developed to assess the direct targets  
563 of predicted transcription factors in *Arabidopsis thaliana* (30). Unlike other methods  
564 of identifying DNA binding sites, DAP-seq has the advantage that chromatin  
565 structure and growth conditions do not play a role in determining transcription  
566 factor binding sites. However, transcription factors that require chromatin structure  
567 or other co-factors to bind to their DNA target site will not be identified by DAP-seq.  
568 Our comparison of ChIP-seq and DAP-seq data for CLR-2 and XLR-1 showed a strong  
569 overlap in these two datasets. Analyses of both datasets were helped substantially  
570 by the availability of RNA-seq data under different carbon sources and by profiling  
571 data of the transcription factor mutants under these same conditions. ~~We may have  
572 missed direct targets of transcription factors using either DAP-seq/RNAseq or  
573 ChIPseq/RNAseq methods due to our stringent differential expression requirements  
574 (at least 2<sup>1-5</sup>-fold) from expression analyses taken at a single time point. Although  
575 we identified 34 TFs whose expression varied across our transcriptional profiling  
576 dataset, mutants in a majority of these TFs did not show an obvious expression  
577 profile difference to wild type when shifted to conditions where their expression~~

578 increased. This result could be due to redundancy of TF function in nutrient  
579 regulation, a role of the TF at a different time point that what was assessed in this  
580 study, or a role in cross regulation that was not obvious from the RNA-seq dataset.  
581 We predict that these TFs do play a role in nutrient regulation in *N. crassa* and that  
582 a combination of DAP-seq to help identify conditions for RNA-seq studies and  
583 expression profiling at additional time points may help to illuminate their function.  
584 We may also have missed direct targets of transcription factors using either DAP-  
585 seq/RNAseq or ChIPseq/RNAseq methods due to our stringent differential expression  
586 requirements (at least 2<sup>1.5</sup>-fold) from expression analyses taken at a single time  
587 point. **Nonetheless**, this approach was particularly helpful in defining the role of  
588 VIB-1 and elucidating additional functions of CRE-1.

589 Our data shows that CRE-1-mediated carbon catabolite repression acts not  
590 only through regulation of PCWDEs and their positive transcription factor regulators,  
591 but also through key sugar catabolic genes and sugar transporters. Repression of  
592 transporter gene expression by CRE-1 reduces entry of signal-transducing sugars  
593 into the cell, thus limiting induction of genes encoding PCWDEs. In *A. niger*, low  
594 concentrations of galacturonic acid were required to induce gene expression of  
595 galacturonic acid utilization genes, including a galacturonic acid transporter, which  
596 was repressed by glucose in a CreA-dependent manner (58). Thus, CRE-1 may be  
597 regulating CCR through more than 4 levels of control or a “quadruple lock”  
598 mechanism: 1. Regulating expression of sugar transporters, 2. Regulating  
599 expression of sugar catabolic genes, 3. Regulating expression of transcription  
600 factors important for expression of genes encoding PCWDEs, and 4. Regulating the  
601 expression of genes encoding PCWDEs (Fig. 4). This “quadruple lock” mechanism  
602 may be important in nutrient sensing, production of PCWDEs based on nutrient  
603 source, and for integration of different nutrient signals for optimal metabolic  
604 regulation during plant biomass deconstruction. Our DAP-seq data on CRE-1  
605 provides a framework for investigating the variety of conditions where CRE-1 plays  
606 a role in regulating metabolism, particularly in conjunction with transcription factors  
607 that control condition-specific responses.

608 The transcription factor VIB-1 belongs to the p53 superfamily, which in  
609 mammalian cells regulates the cell cycle, DNA repair, and apoptosis (59). In  
610 *Saccharomyces cerevisiae*, the p53 homolog, Ndt80, regulates entry into meiosis  
611 upon nitrogen starvation (60). The genome of *N. crassa* has three p53 homologs,

612 *vib-1*, *fsd-1* and NCU04729, none of which are required for meiosis, although both  
613 *fsd-1* and *vib-1* mutants affect female reproductive structure development, which is  
614 regulated by nutritional status (61). In other filamentous fungi, *vib-1* homologs have  
615 been shown to regulate protease production, production of extracellular hydrolases  
616 and PCWDEs, N-acetyl glucosamine catabolism, and secondary metabolism (62).  
617 Additionally, a *vib-1* homolog in the human pathogen *Candida albicans* regulates  
618 virulence (63). These observations suggest a general role for VIB-1 orthologs in  
619 sensing and responding to the availability of nutrients in their environment. Upon  
620 starvation, VIB-1 is required for an increase in the expression of a number of  
621 secreted proteins associated with polysaccharide and protein degradation (VIB-1  
622 core regulon). These “scout” enzymes release mono-/di-/oligosaccharides, which are  
623 transported into the cell, resulting in full activation of genes and secretion of  
624 enzymes associated with the utilization of a particular plant biomass component.  
625 This model is consistent with VIB-1 functioning as a general starvation response  
626 transcription factor, or a transcription factor important for basal expression of  
627 nutrient acquisition genes. In cells lacking VIB-1, a positive feedback loop is not fully  
628 initiated, and full expression PCWDE genes necessary for optimal utilization of plant  
629 biomass is not achieved. Also consistent with this model, is that *vib-1* is not under  
630 carbon catabolite repression regulation, as VIB-1 and its direct target genes are not  
631 regulated by CRE-1.

632         Previously, it was hypothesized that VIB-1 functions upstream of CRE-1 and  
633 COL-26, as the introduction of  $\Delta cre-1 \Delta col-26$  mutations into a  $\Delta vib-1$  mutant  
634 suppressed the inability of the  $\Delta vib-1$  mutant to utilize cellulose (21). Our DAP-seq  
635 and RNA-seq data supports an alternative hypothesis. We predict that the deletion  
636 of *cre-1* and *col-26* allows sufficient expression of *clr-2* to restore growth of the  $\Delta vib-$   
637 *1* mutant on cellulose (partly due to lack of repression of the cellodextrin  
638 transporters by CRE-1) in a manner similar to how deletion of the three  $\beta$ -  
639 glucosidase genes ( $\Delta 3BG$ ) restored cellulase production in the  $\Delta vib-1$  mutant on  
640 cellobiose (48). Under carbon-limiting conditions, VIB-1 promotes expression of *clr-2*  
641 and *pdr-2* along with a small set of PCWDEs. These secreted enzymes cleave plant  
642 biomass and signaling sugars are transported into the cell. For cellulose utilization,  
643 cellobiose (or a modified version of cellobiose) results in inactivation of the  
644 repressor CLR-3 (48), allowing activation of CLR-1. CLR-1 promotes expression of  
645 *clr-2* and cellulases, and together with VIB-1, results in full expression of *clr-2* and

646 induction of a positive feedback loop. As the glucose concentration increases inside  
647 the cell, CRE-1 mediated CCR is activated, reducing expression of *clr-1* and  
648 cellodextrin transporters *cdt-1*, *cdt-2*, and *cbt-1*, thus negatively regulating  
649 expression of PCWDEs both by limiting the expression of *clr-1* and the cleaving and  
650 import of sugar signaling molecules (Fig. 4). Our data supports the cooperative  
651 regulation of PCWDEs by negative regulation of transporters by CRE-1 and positive  
652 regulation of enzyme scouts that regulate signaling processes via VIB-1.

653 VIB-1 regulation of HET domain genes may also play a role in nutrient  
654 acquisition. HET domain genes allow fungi to distinguish between self and non-self  
655 cells, and initiate programmed cell death upon fusion of non-self pairs (64).  
656 Starvation increases vegetative cell fusion frequency in a number of ascomycete  
657 fungi, including *N. crassa* (65-67). We hypothesize that VIB-1 increases expression  
658 of these HET domain genes to ensure viable fusion is prevented between non-self  
659 cells. Potentially, this activity may also be related to the regulation of secondary  
660 metabolism by VIB-1-like proteins. The promoters of LaeA-like methyltransferase  
661 domain containing proteins were abundant in the direct target gene set of VIB-1.  
662 LaeA and LaeA-like methyltransferase orthologs are negative regulators of secondary  
663 metabolite production in fungi (47, 68, 69). The modulation of the expression of  
664 these methyltransferases by VIB-1 may have downstream gene regulatory  
665 consequences that may affect competition among microbes and nutrient acquisition  
666 during plant biomass deconstruction and utilization.

667

## 668 **Materials and Methods**

### 669 **Comprehensive list of PCWDE genes in the *N. crassa* genome.**

670 A comprehensive list of predicted *N. crassa* genes encoding PCWDE was  
671 compiled by examining all CAZymes from the Carbohydrate Active Enzymes  
672 Database (<http://www.cazy.org>) (70) (Table S2).

673

### 674 **Strains, Growth Conditions, RNA extraction and RNA-seq**

675 Strains are listed in Table S5 (see Supplemental material and Methods for  
676 strain construction). For RNAseq experiments induction conditions, 2mM mono and  
677 disaccharides were used (23); for complex polysaccharides and plant biomass 1%  
678 (w/v) was used (Table S1). RNA isolation and RNA-seq methods are as-described in  
679 {Supplemental Materials and Methods}. Filtered reads were mapped against *N.*

680 *crassa* OR74A genome (v12) using Tophat 2.0.4 (71) and transcript abundance was  
681 estimated with Cufflinks 2.0.2 (72) in fragments per kilobase of transcript per million  
682 mapped reads (FPKMs) using upper quartile normalization. [Differential expression  
683 analysis was performed on raw counts with DEseq2 version 3.3 \(Love MI, Huber W,  
684 & Anders S \(2014\) Moderated estimation of fold change and dispersion for RNA-seq  
685 data with DESeq2. \*Genome Biol\* 15:550\) using data from biological triplicates.](#) Data  
686 available at:  
687 <https://genome.jgi.doe.gov/portal/TheFunENCproject/TheFunENCproject.info.html>.  
688 <https://www.ncbi.nlm.nih.gov/sra> **submission in progress.**

### 689 **Weighted Correlation Network Analysis (WGCNA) and FUNCAT** 690 **analyses**

692 The gene co-expression network was calculated across expression profiles for  
693 the wild-type strain exposed to carbon sources listed in Dataset S1 using the R  
694 package WGCNA (26) and a custom catalogue (11) based on MPS Functional  
695 Catalogue Database (FuncatDB) (73) with expanded categories for cell wall  
696 degradation-related genes for enrichment analysis.

### 697 **Enzyme activity and transport assays**

699 WT and  $\Delta cre-1$  strains were induced in 0.5% pectin or 0.5% pectin plus 2% D-  
700 glucose and transferred to either 100  $\mu$ M L-rhamnose or 100  $\mu$ M L-rhamnose plus  
701 100  $\mu$ M D-glucose as uptake solution. WT and  $\Delta sut-28$  strains were transferred to  
702 uptake solutions containing either 100  $\mu$ M L-rhamnose, 90  $\mu$ M D-fucose (VWR,  
703 A16789), 90  $\mu$ M D-xylose or 90  $\mu$ M D-galactose (Sigma Aldrich, G0750).  
704 Monosaccharide concentration of sample supernatants was quantified by high pH  
705 Anion Exchange Chromatography - Pulsed Amperometric Detection (HPAEC-PAD) on  
706 an ICS-3000 instrument (Thermo Scientific, USA). A 25  $\mu$ l sample was injected onto  
707 a Dionex CarboPac PA20 column (3  $\times$  30 mm guard and 3  $\times$  150 mm analytical) and  
708 eluted using an isocratic mobile phase of 10 mM NaOH at 0.4 ml/min and 30°C over  
709 12 min. Cellulase activity assays were modified from Coradetti *et al* (27) (see  
710 Supplemental Material and Methods).

### 711 **DAP-seq**

713 Predicted open reading frames for each transcription factor were amplified  
714 from cDNA generated using RNA to cDNA EcoDry premix (Clontech). Amplified  
715 transcription factor sequences were inserted into an expression vector containing  
716 T7 and SP6 promoters upstream of HALO tag as previously described (30).

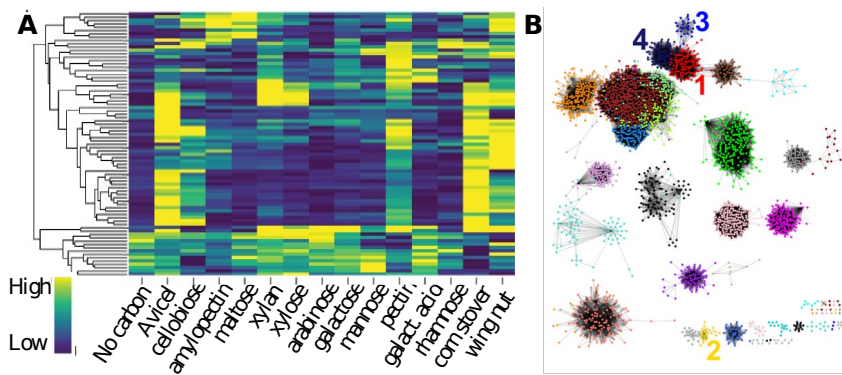
717 *In vitro* transcription and translation of transcription factors was performed  
718 using Promega TnT T7 Rabbit Reticulocyte Quick Coupled Transcription/Translation  
719 System by incubating 1ug of plasmid DNA with 60ul of TnT Master Mix and 1.5ul of  
720 1mM methionine overnight at room temperature. Expression was verified using  
721 Western blot analysis with Promega Anti-HaloTag monoclonal antibody. Single DAP-  
722 seq libraries were generated once for each transcription factor tested and  
723 sequenced once with Illumina MiSeq 2x150BP runs.

724 Filtered reads were aligned to *N. crassa* OR74A genome (v12) using Bowtie2  
725 v2.3.2 (71). Peak calling was performed using MACS2 v2.1.1 (74) with p-value cutoff  
726 at 0.001 and utilizing negative control library alignments. Peaks within 3000 bp  
727 upstream of translation start sites were selected for and annotated using a custom  
728 python script. The same python script was used for reanalysis of ChIP-seq peaks  
729 dataset from Craig et al. 2015 (10) for DAP-seq/ChIPseq comparisons. DAP-seq data  
730 available at: <https://www.ncbi.nlm.nih.gov/sra/SRP133627>.

731

732





733

734

735

736

737

738

739

740

741

742 **Figure 1. Hierarchical clustering and weighted gene co-expression network**

743 **analysis of *N. crassa* transcriptome across carbon sources.** (A) Hierarchical

744 clustering of of the normalized counts (FPKM) expression patterns of genes

745 encoding PCWDEs in cells shifted to indicated carbon sources. All di- and

746 monosaccharides are at 2mM concentration and complex carbohydrates are 1% W/

747 V. Color bar represents the spectrum from lowest normalized count to highest

748 normalized count for each gene centered on mean expression. (B) Co-expression

749 network with nodes representing genes colored by modules and edges between

750 genes with correlated expression profiles, shown using Cytoscape (75) (SI Dataset

751 2). Four modules enriched in genes encoding PCWDEs and polysaccharide

752 metabolism are labeled. Module 1 (red): genes associated cellulose and

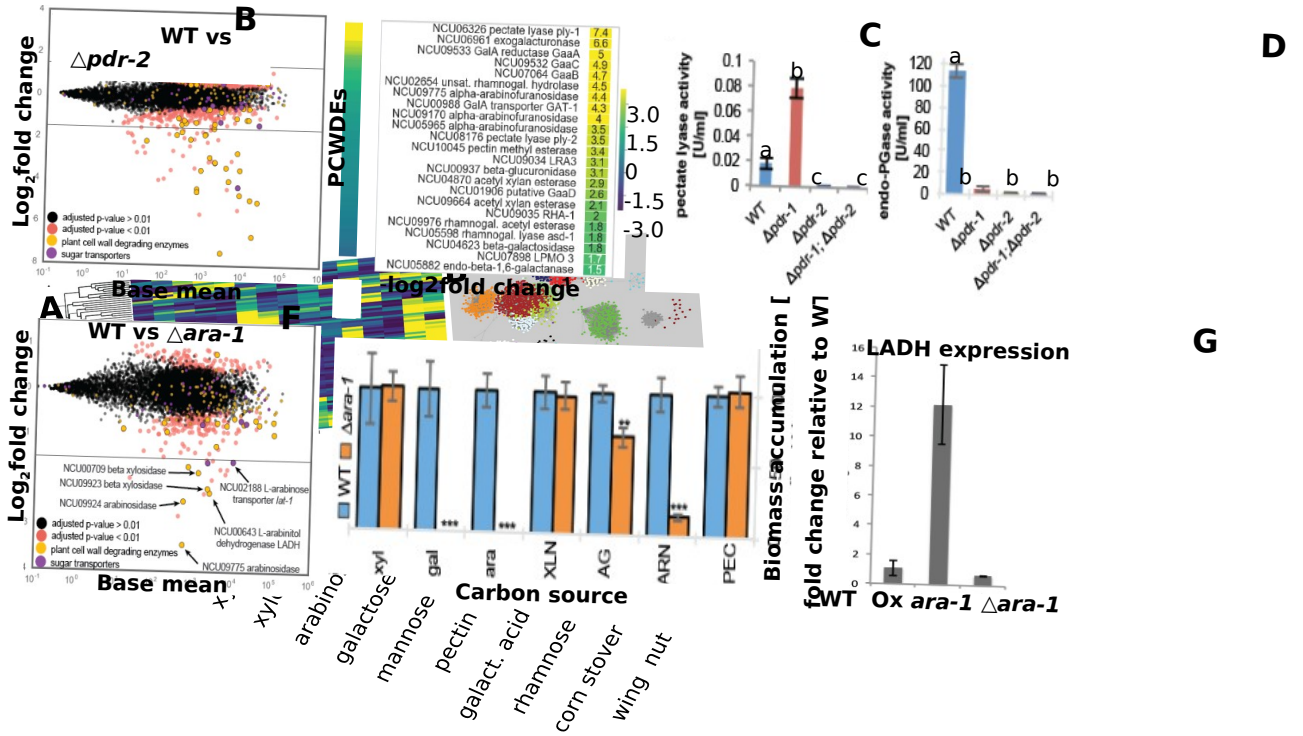
753 hemicellulose utilization. Module 2 (yellow): genes associated with pectin

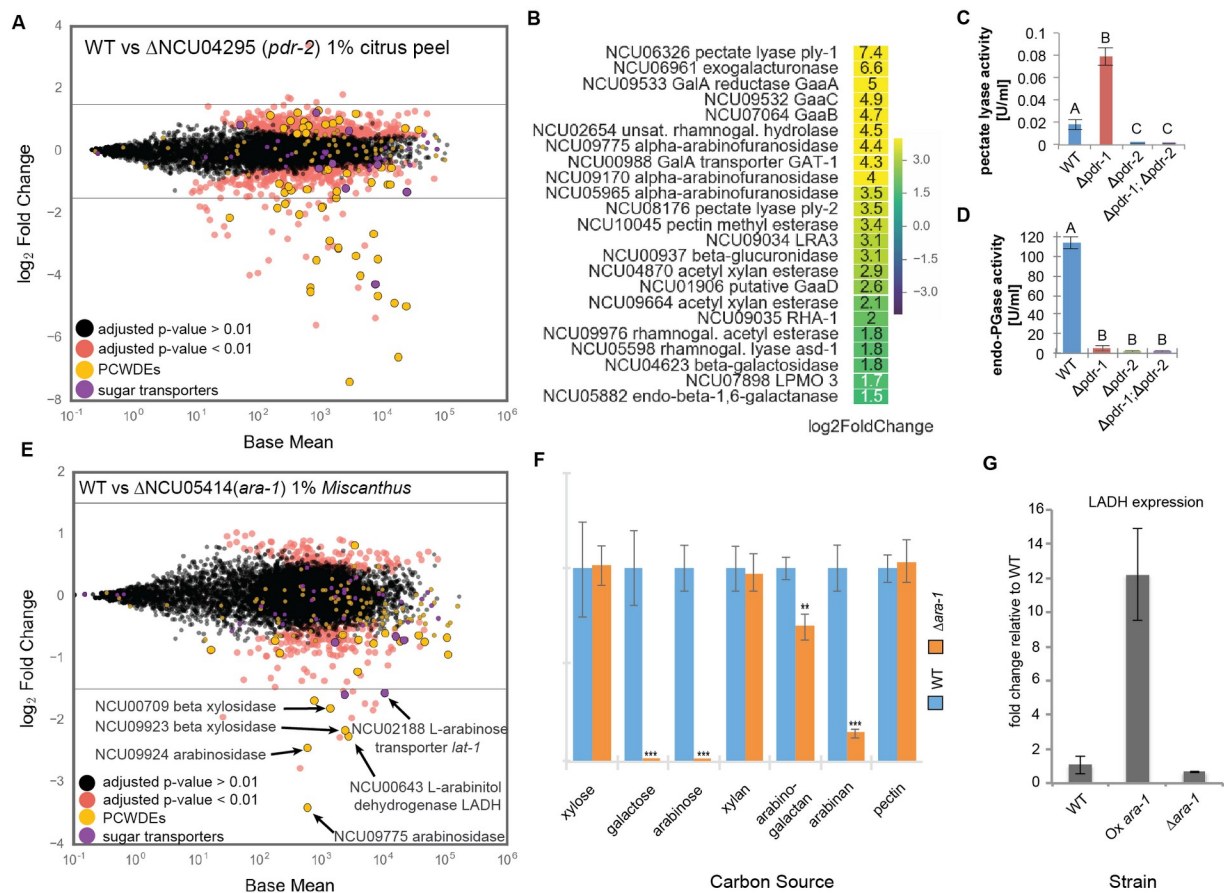
754 deconstruction. Module 3 (blue): pentose catabolic and xylan utilization genes.

755 Module 4 (midnight blue): genes encoding ER and protein processing proteins (SI

756 Dataset 2). Total number of genes shown in the network is 3,282.

757





759

760 **Figure 2. The transcription factor *pdr-2* regulates pectin degradation and**

761 **the transcription factor *ara-1* regulates arabinose utilization.** (A) Differential

762 expression analysis of  $\Delta$ NCU04295 (*pdr-2*) relative to wild type cells after a shift to

763 1% w/v citrus peel (SI Dataset 1). PCWDEs are yellow and sugar transporters are

764 purple. “Base mean” is the mean of normalized counts for triplicates of both

765 conditions tested. (B) Differential expression of PCWDEs ranked by degree of  $\log_2$

766 fold change from (A). (C) pectate lyase and (D) endo-polygalacturonanase (endo-

767 PGase) activities of  $\Delta$ *pdr-1*,  $\Delta$ *pdr-2* and  $\Delta$ *pdr-1*  $\Delta$ *pdr-2* mutants relative to WT. Error

768 bars represent standard deviation (n = 3). Significance was determined by ANOVA

769 followed by a post-hoc Tukey’s test. The letters above each bar indicate statistical

770 significance with a mean difference of p < 0.05. (E) Differential expression analysis

771 of  $\Delta$ NCU05414 (*ara-1*) in comparison to WT after cultures were shifted to 1% w/v

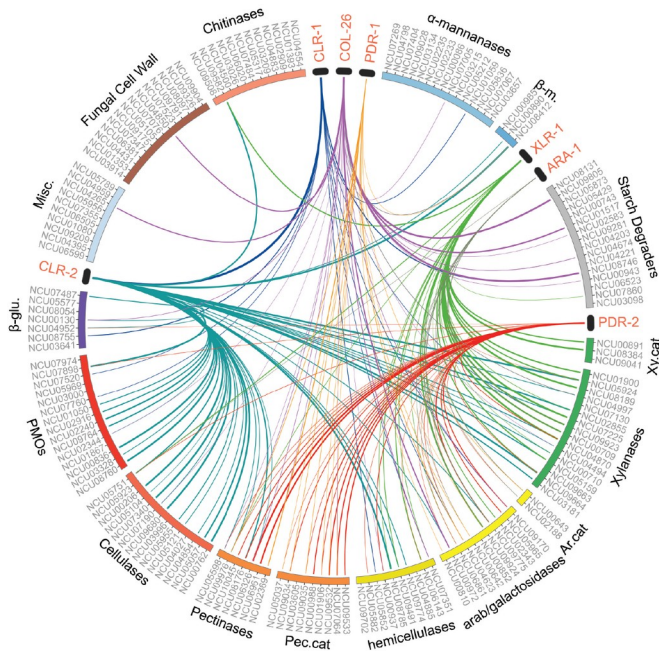
772 *Miscanthus* (SI Dataset 1). PCWDEs are in yellow and sugar transporters are in

773 purple. “Base mean” is the mean of normalized counts for triplicates of both

774 conditions tested. (F) Relative biomass accumulation of  $\Delta$ *ara-1* normalized to WT

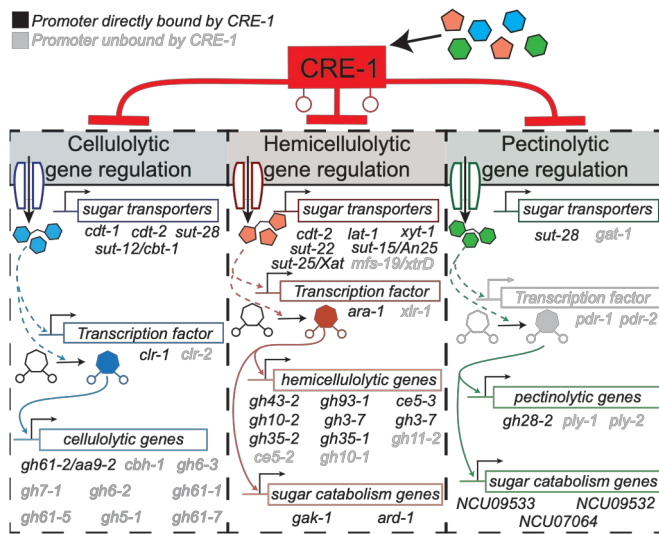
775 cultured in the indicated carbon sources. Significance was determined by an

776 independent two-sample t-test of WT against  $\Delta ara-1$  with  $**p < 0.01$  and  $***p <$   
 777  $0.001$  ( $n=3$ ). (G) Relative *ard-1* (L-arabinitol dehydrogenase: LADH) expression  
 778 relative to *act* after shift to arabinose in  $\Delta ara-1$  and in an *ara-1* overexpression  
 779 strain (*Ox ara-1*). For D, F and G, error bars represent standard deviation ( $n >=3$ ).  
 780 .



781  
 782 **Figure 3. Overlapping regulons of major PCWDE regulators in *N. crassa*.**  
 783 Plot built with Circos v0.69 (76) to display positive regulation of catabolic CAZymes  
 784 by indicated transcription factors (red) [\(SI Dataset 1\)](#). [RNA-seq data for all TFs was](#)  
 785 [obtained under identical culture conditions \(see materials and methods\)](#). CAZymes  
 786 are divided into functional groups displayed on the outer edge of the plot. Pec. cat”  
 787 pectin catabolism, “Ar” arabinose, “Ar. cat.” Arabinose catabolism, “Xy” xylose and  
 788 “β-m” for β-mannanases, β-glu for β-glucosidases, PMO, polysaccharide  
 789 monooxygenases. Each CAZyme is represented by its gene ID. Each line represents  
 790 genes with significantly different expression between WT and a transcription factor  
 791 deletion mutant under the following conditions:  $\Delta clr-1$  and  $\Delta clr-2$  shifted to 1%  
 792 Avicel,  $\Delta col-26$  shifted to 2mM maltose [\(Yi\)](#),  $\Delta pdr-1$  shifted to 1% pectin [\(Thieme\)](#),  
 793  $\Delta pdr-2$  shifted to 1% citrus peel,  $\Delta ara-1$  shifted to 1% *Miscanthus*, and  $\Delta xlr-1$  shifted  
 794 to 1% xylan [\(SI Dataset 3\)](#). The thickness of the line corresponds to degree of fold  
 795 change in the transcription factor deletion mutants as compared to wild type cells  
 796 (11, 19) [\(SI Dataset 3\)](#).





798

799

800 **Figure 4. CRE-1-mediated carbon catabolite repression acts through sugar**  
 801 **transporter, transcription factor, sugar catabolism, and PCWDE**

802 **regulate plant cell wall degradation.** CRE-1 regulates expression of PCWDE

803 regulons by repressing expression of sugar transporters, transcription factors, and

804 genes involved in the utilization of plant biomass components. Sugars transported

805 into the cell may play either a direct or indirect role in the activation of transcription

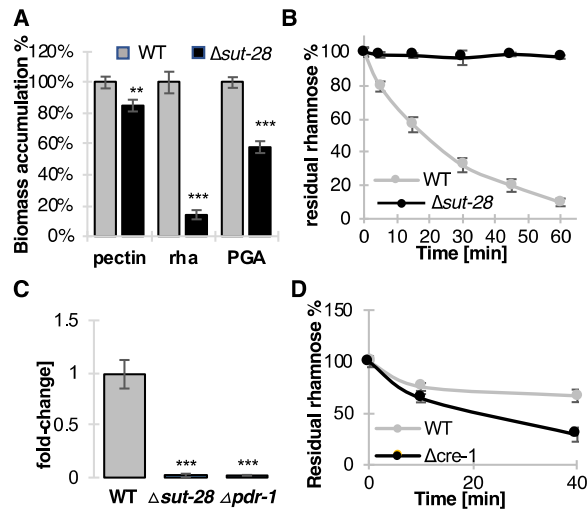
806 factors necessary for cellulolytic, hemicellulolytic, and pectinolytic gene expression.

807 The promoters of genes in black are directly bound by CRE-1, and the promoters of

808 genes in grey are not bound by CRE-1. Blue, orange, and green arrows indicate

809 regulation that occurs downstream of CRE-1-mediated repression.

810



811

812

813 **Figure 5. *sut-28* expression and rhamnose transport activity in wild type**

814 **and  $\Delta cre-1$  strains.** (A) Relative biomass of FGSC2489 (WT) and  $\Delta sut-28$  strains

815 incubated in pectin, rhamnose, and polygalacturonic acid as determined by dry

816 weight. (B) Rhamnose uptake in FGSC2489 and  $\Delta sut-28$  strains after induction on

817 pectin. (C) Relative NCU09034 (L-rhamnonate dehydratase) expression relative to

818 *act* in FGSC2489,  $\Delta sut-28$ , and  $\Delta pdr-1$  after induction on rhamnose. (D) Rhamnose

819 uptake in FGSC2489 and  $\Delta cre-1$  strains induced with pectin plus glucose. Error bars

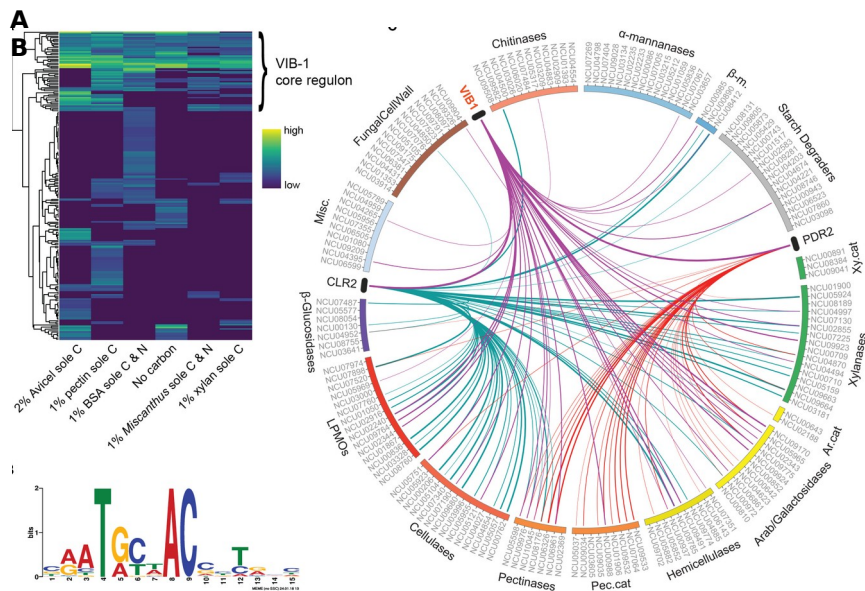
820 represent standard deviation ( $n \geq 3$ ). Significance was determined by an

821 independent two-sample t-test of WT against  $\Delta ara-1$  with  $**p < 0.01$  and  $***p <$

822 0.001.

823





824

825

826 **Figure 6. VIB-1 regulon.** (A) Hierarchical clustering of  $\log_2$  fold change values  
 827 from differential expression analysis of FGSC2489 versus  $\Delta vib-1$  strains shifted to  
 828 the indicated carbon conditions. Only genes with greater than  $2^{1.5}$ -fold change and  
 829 with promoters bound by VIB-1 via DAP-seq are included. The VIB-1 core regulon is  
 830 a cluster of genes that were differentially expressed across multiple conditions (SI  
 831 Dataset 5). (B) VIB-1 binding motif built using MEME v4.12.0 using DAP binding peak  
 832 sequences of VIB-1 core regulon. E-value =  $1.8^{-89}$ . (C) Plot built with Circos v0.69  
 833 (76) to display positive regulation of a catabolic CAZymes by VIB-1 and the  
 834 transcription factors CLR-1 and PDR-2, which are bound and directly regulated by  
 835 VIB-1. The thickness of the line corresponds to degree of fold change between WT  
 836 and transcription factor mutant (SI Dataset 3 and 5).

837

### 838 Acknowledgements

839 [We acknowledge the use of deletion strains generated by grant P01 GM-068087](#)  
 840 [“Functional Analysis of a Model Filamentous Fungus,”](#) and which are publicly  
 841 [available at the Fungal](#)  
 842 [Genetics Stock Center.](#) This work was supported by an Energy Biosciences Institute  
 843 Grant, ~~to N.L.G.~~ and a Laboratory Directed Research and Development Program of  
 844 Lawrence Berkeley National Laboratory under US Department of Energy Contract  
 845 DE-AC02-05CH11231 [and funds from the Fred E. Dickinson Chair of Wood Science](#)  
 846 [and Technology to N.L.G.](#) -V.W.W was [partially](#) supported by a National Institutes



847 | of Health NRSA Trainee Grant 5T32GM007127-39. We thank ~~the Fungal Genetics~~  
848 | ~~Stock Center for strains and~~ Elias Bleek (TUMS) for assistance with transporter  
849 | assays.

850 | V.W.W., N.T., L.B.H., A.D., D.J.K., J.L., V.S., A.L., R.M. and M.J.B. performed  
851 | experiments. V.W.W., S.C. and Y.X. performed computational analyses. V.W.W.,  
852 | J.P.B., R.C.O., I.V.G. and N.L.G. were involved in study conception and design.  
853 | V.W.W., N.T., L.B.H., J.P.B. and N.L.G. wrote and edited the manuscript.

854 |

## 855 | **References ~~NOT UPDATED~~**

- 856 | 1. Fernandez CW & Kennedy PG (2016) Revisiting the 'Gadgil effect': do  
857 | interguild fungal interactions control carbon cycling in forest soils? *New*  
858 | *Phytol* 209:1382-1394.
- 859 | 2. Gupta VK, *et al.* (2016) Fungal enzymes for bio-products from sustainable and  
860 | waste biomass. *Trends Biochem Sci* 41:633-645.
- 861 | 3. Caffall KH & Mohnen D (2009) The structure, function, and biosynthesis of  
862 | plant cell wall pectic polysaccharides. *Carbohyd Res* 344:1879-1900.
- 863 | 4. Ragauskas AJ, *et al.* (2014) Lignin valorization: improving lignin processing in  
864 | the biorefinery. *Science* 344:1246843.
- 865 | 5. Kunitake E & Kobayashi T (2017) Conservation and diversity of the regulators  
866 | of cellulolytic enzyme genes in Ascomycete fungi. *Curr Genet* 63:951-958.
- 867 | 6. Huberman LB, Liu J, Qin L, & Glass NL (2016) Regulation of the  
868 | lignocellulolytic response in filamentous fungi. *Fungal Biol Rev* 30:101-111.
- 869 | 7. Furukawa T, *et al.* (2009) Identification of specific binding sites for XYR1, a  
870 | transcriptional activator of cellulolytic and xylanolytic genes in *Trichoderma*  
871 | *reesei*. *Fungal Genet Biol* 46:564-574.
- 872 | 8. Hasper AA, Trindade LM, van der Veen D, van Ooyen AJ, & de Graaff LH  
873 | (2004) Functional analysis of the transcriptional activator XlnR from  
874 | *Aspergillus niger*. *Microbiol* 150:1367-1375.
- 875 | 9. Brunner K, Lichtenauer AM, Kratochwill K, Delic M, & Mach RL (2007) Xyr1  
876 | regulates xylanase but not cellulase formation in the head blight fungus  
877 | *Fusarium graminearum*. *Curr Genet* 52:213-220.
- 878 | 10. Craig JP, Coradetti ST, Starr TL, & Glass NL (2015) Direct target network of  
879 | the *Neurospora crassa* plant cell wall deconstruction regulators CLR-1, CLR-2,  
880 | and XLR-1. *MBio* 6(5).
- 881 | 11. Thieme N, *et al.* (2017) The transcription factor PDR-1 is a multi-functional  
882 | regulator and key component of pectin deconstruction and catabolism in  
883 | *Neurospora crassa*. *Biotechnol Biofuels* 10:149.
- 884 | 12. Gruben BS, *et al.* (2014) *Aspergillus niger* RhaR, a regulator involved in L-  
885 | rhamnose release and catabolism. *Appl Microbiol Biotechnol* 98:5531-5540.
- 886 | 13. Alazi E, *et al.* (2016) The transcriptional activator GaaR of *Aspergillus niger* is  
887 | required for release and utilization of d-galacturonic acid from pectin. *FEBS*  
888 | *Lett* 590:1804-1815.
- 889 | 14. Zhang L, *et al.* (2016) A novel Zn<sup>2</sup> Cys<sup>6</sup> transcription factor BcGaaR regulates  
890 | D-galacturonic acid utilization in *Botrytis cinerea*. *Mol Microbiol* 100:247-262.

- 891 15. Battaglia E, *et al.* (2011) Analysis of regulation of pentose utilisation in  
892 *Aspergillus niger* reveals evolutionary adaptations in Eurotiales. *Stud Mycol*  
893 69:31-38.
- 894 16. Klaubauf S, Zhou M, Lebrun MH, de Vries RP, & Battaglia E (2016) A novel L-  
895 arabinose-responsive regulator discovered in the rice-blast fungus *Pyricularia*  
896 *oryzae* (*Magnaporthe oryzae*). *FEBS Lett* 590:550-558.
- 897 17. Sun J & Glass NL (2011) Identification of the CRE-1 cellulolytic regulon in  
898 *Neurospora crassa*. *PLoS One* 6:e25654.
- 899 18. Ries LN, Beattie SR, Espeso EA, Cramer RA, & Goldman GH (2016) Diverse  
900 regulation of the CreA carbon catabolite repressor in *Aspergillus nidulans*.  
901 *Genetics* 203:335-352.
- 902 19. Xiong Y, *et al.* (2017) A fungal transcription factor essential for starch  
903 degradation affects integration of carbon and nitrogen metabolism. *PLoS*  
904 *Genet* 13:e1006737.
- 905 20. Nitta M, *et al.* (2012) A new Zn(II)(2)Cys(6)-type transcription factor BgIR  
906 regulates beta-glucosidase expression in *Trichoderma reesei*. *Fungal Genet*  
907 *Biol* 49:388-397.
- 908 21. Xiong Y, Sun J, & Glass NL (2014) VIB1, a link between glucose signaling and  
909 carbon catabolite repression, is essential for plant cell wall degradation in  
910 *Neurospora crassa*. *PLoS Genet* 10:e1004500.
- 911 22. Ivanova C, *et al.* (2017) Genome sequencing and transcriptome analysis of  
912 *Trichoderma reesei* QM9978 strain reveals a distal chromosome translocation  
913 to be responsible for loss of *vib1* expression and loss of cellulase induction.  
914 *Biotechnol Biofuels* 10:209.
- 915 23. Znameroski EA, *et al.* (2012) Induction of lignocellulose-degrading enzymes in  
916 *Neurospora crassa* by cellodextrins. *Proc Natl Acad Sci USA* 109:6012-6017.
- 917 24. Gielkens MM, Dekkers E, Visser J, & de Graaff LH (1999) Two  
918 cellobiohydrolase-encoding genes from *Aspergillus niger* require D-xylose and  
919 the xylanolytic transcriptional activator XlnR for their expression. *Appl*  
920 *Environ Microbiol* 65:4340-4345.
- 921 25. Saier MH, Jr., *et al.* (2016) The transporter classification database (TCDB):  
922 recent advances. *Nucleic Acids Res* 44:D372-379.
- 923 26. Langfelder P & Horvath S (2008) WGCNA: an R package for weighted  
924 correlation network analysis. *BMC Bioinformatics* 9:559.
- 925 27. Coradetti ST, *et al.* (2012) Conserved and essential transcription factors for  
926 cellulase gene expression in ascomycete fungi. *Proc Natl Acad Sci USA*  
927 109:7397-7402.
- 928 28. Benz JP, *et al.* (2014) A comparative systems analysis of polysaccharide-  
929 elicited responses in *Neurospora crassa* reveals carbon source-specific  
930 cellular adaptations. *Mol Microbiol* 91:275-299.
- 931 29. Benocci T, *et al.* (2018) ARA1 regulates not only l-arabinose but also d-  
932 galactose catabolism in *Trichoderma reesei*. *FEBS Lett* 592:60-70.
- 933 30. O'Malley RC, *et al.* (2016) Cistrome and epicistrome features shape the  
934 regulatory DNA landscape. *Cell* 165:1280-1292.
- 935 31. Derntl C, *et al.* (2013) Mutation of the Xylanase regulator 1 causes a glucose  
936 blind hydrolase expressing phenotype in industrially used *Trichoderma*  
937 strains. *Biotechnol Biofuels* 6:62.
- 938 32. Adnan M, *et al.* (2017) Carbon catabolite repression in filamentous fungi. *Int J*  
939 *Mol Sci* 19(1).

- 940 33. Espeso EA & Penalva MA (1994) In vitro binding of the two-finger repressor  
941 CreA to several consensus and non-consensus sites at the *ipnA* upstream  
942 region is context dependent. *FEBS Lett* 342:43-48.
- 943 34. Tamayo EN, et al. (2008) CreA mediates repression of the regulatory gene  
944 *xlnR* which controls the production of xylanolytic enzymes in *Aspergillus*  
945 *nidulans*. *Fungal Genet Biol* 45:984-993.
- 946 35. Wang B, et al. (2017) Identification and characterization of the glucose dual-  
947 affinity transport system in *Neurospora crassa*: pleiotropic roles in nutrient  
948 transport, signaling, and carbon catabolite repression. *Biotechnol Biofuels*  
949 10:17.
- 950 36. Galazka JM, et al. (2010) Cellodextrin transport in yeast for improved biofuel  
951 production. *Science* 330:84-86.
- 952 37. Xiong Y, et al. (2014) The proteome and phosphoproteome of *Neurospora*  
953 *crassa* in response to cellulose, sucrose and carbon starvation. *Fungal Genet*  
954 *Biol* 72:21-33.
- 955 38. Li X, et al. (2015) Cellobionic acid utilization: from *Neurospora crassa* to  
956 *Saccharomyces cerevisiae*. *Biotechnol Biofuels* 8:120.
- 957 39. Li X, et al. (2015) Expanding xylose metabolism in yeast for plant cell wall  
958 conversion to biofuels. *eLife* 4.
- 959 40. Znameroski EA, et al. (2014) Evidence for transeptor function of cellodextrin  
960 transporters in *Neurospora crassa*. *J Biol Chem* 289:2610-2619.
- 961 41. Du J, Li S, & Zhao H (2010) Discovery and characterization of novel d-xylose-  
962 specific transporters from *Neurospora crassa* and *Pichia stipitis*. *Mol Biosyst*  
963 6:2150-2156.
- 964 42. Li J, Lin L, Li H, Tian C, & Ma Y (2014) Transcriptional comparison of the  
965 filamentous fungus *Neurospora crassa* growing on three major  
966 monosaccharides D-glucose, D-xylose and L-arabinose. *Biotechnol Biofuels*  
967 7:31.
- 968 43. Sloothak J, Odoni DI, Martins Dos Santos VA, Schaap PJ, & Tamayo-Ramos JA  
969 (2016) Identification of a novel L-rhamnose uptake transporter in the  
970 filamentous fungus *Aspergillus niger*. *PLoS Genet* 12:e1006468.
- 971 44. Dementhon K, Iyer G, & Glass NL (2006) VIB-1 is required for expression of  
972 genes necessary for programmed cell death in *Neurospora crassa*. *Eukaryot*  
973 *Cell* 5:2161-2173.
- 974 45. Xiang Q & Glass NL (2002) Identification of *vib-1*, a locus involved in  
975 vegetative incompatibility mediated by *het-c* in *Neurospora crassa*. *Genetics*  
976 162:89-101.
- 977 46. Zhao J, et al. (2015) Identification of allorecognition loci in *Neurospora crassa*  
978 by genomics and evolutionary approaches. *Mol Biol Evol* 32:2417-2432.
- 979 47. Bok JW & Keller NP (2004) *LaeA*, a regulator of secondary metabolism in  
980 *Aspergillus* spp. *Eukaryot Cell* 3:527-535.
- 981 48. Huberman LB, Coradetti ST, & Glass NL (2017) Network of nutrient-sensing  
982 pathways and a conserved kinase cascade integrate osmolarity and carbon  
983 sensing in *Neurospora crassa*. *Proc Natl Acad Sci USA* 114:E8665-E8674.
- 984 49. Katz ME, Gray K-A, & Cheetham BF (2006) The *Aspergillus nidulans xprG*  
985 (*phoG*) gene encodes a putative transcriptional activator involved in the  
986 response to nutrient limitation. *Fungal Genet Biol* 43:190.
- 987 50. Mittenhuber G (2001) Phylogenetic analyses and comparative genomics of  
988 vitamin B6 (pyridoxine) and pyridoxal phosphate biosynthesis pathways. *J Mol*  
989 *Microbiol Biotechnol* 3:1-20.

- 990 51. Casado Lopez S, et al. (2018) Induction of genes encoding plant cell wall-  
991 degrading carbohydrate-active enzymes by lignocellulose-derived  
992 monosaccharides and cellobiose in the white-rot fungus *Dichomitus squalens*.  
993 *Appl Environ Microbiol* 84(11).
- 994 52. Zhang W, et al. (2013) Two major facilitator superfamily sugar transporters  
995 from *Trichoderma reesei* and their roles in induction of cellulase biosynthesis.  
996 *J Biol Chem*. 288:32861-72.
- 997 53. Brienzo M, Monte JR, & Milagres AM (2012) Induction of cellulase and  
998 hemicellulase activities of *Thermoascus aurantiacus* by xylan hydrolyzed  
999 products. *World J Microbiol Biotechnol* 28:113-119.
- 1000 54. Schape P, et al. (2019) Updating genome annotation for the microbial cell  
1001 factory *Aspergillus niger* using gene co-expression networks. *Nucleic Acids*  
1002 *Res* 47:559-569.
- 1003 55. Benz JP, et al. (2014) A comparative systems analysis of polysaccharide-  
1004 elicited responses in *Neurospora crassa* reveals carbon source-specific  
1005 cellular adaptations. *Mol Microbiol* 91:275-99.
- 1006 56. Seiboth B & Metz B (2011) Fungal arabinan and L-arabinose metabolism. *Appl*  
1007 *Microbiol Biotechnol* 89:1665-1673.
- 1008 57. Mojzita D, Herold S, Metz B, Seiboth B, & Richard P (2012) L-xylo-3-hexulose  
1009 reductase is the missing link in the oxidoreductive pathway for D-galactose  
1010 catabolism in filamentous fungi. *J Biol Chem* 287:26010-26018.
- 1011 58. Niu J, et al. (2015) The interaction of induction and repression mechanisms in  
1012 the regulation of galacturonic acid-induced genes in *Aspergillus niger*. *Fungal*  
1013 *Genet Biol* 82:32-42.
- 1014 59. Haupt S, Louria-Hayon I, & Haupt Y (2003) P53 licensed to kill? Operating the  
1015 assassin. *J Cell Biochem*. 88:76-82.
- 1016 60. Xu L, Ajimura M, Padmore R, Klein C, & Kleckner N (1995) NDT80, a meiosis-  
1017 specific gene required for exit from pachytene in *Saccharomyces cerevisiae*.  
1018 *Mol Cell Biol* 15:6572-6581.
- 1019 61. Hutchison EA & Glass NL (2010) Meiotic regulators Ndt80 and IME-2 have  
1020 different roles in *Saccharomyces* and *Neurospora*. *Genetics* 185:1271-1282.
- 1021 62. Katz ME (2019) Nutrient sensing-the key to fungal p53-like transcription  
1022 factors? *Fungal Genet Biol* 124:8-16.
- 1023 63. Min K, Biermann A, Hogan DA, & Konopka JB (2018) Genetic analysis of  
1024 NDT80 family transcription factors in *Candida albicans* using new CRISPR-  
1025 Cas9 approaches. *mSphere* 3(6).
- 1026 64. Daskalov A, Heller J, Herzog S, Fleissner A, & Glass NL (2017) Molecular  
1027 mechanisms regulating cell fusion and heterokaryon formation in filamentous  
1028 fungi. *Microbiol Spectr* 5(2).
- 1029 65. Roca MG, Weichert M, Siegmund U, Tudzynski P, & Fleissner A (2012)  
1030 Germling fusion via conidial anastomosis tubes in the grey mould *Botrytis*  
1031 *cinerea* requires NADPH oxidase activity. *Fungal Biol* 116:379-387.
- 1032 66. Ishikawa FH, Souza EA, Read ND, & Roca MG (2010) Live-cell imaging of  
1033 conidial fusion in the bean pathogen, *Colletotrichum lindemuthianum*. *Fungal*  
1034 *Biol* 114:2-9.
- 1035 67. Fischer-Harman V, Jackson KJ, Munoz A, Shoji JY, & Read ND (2012) Evidence  
1036 for tryptophan being a signal molecule that inhibits conidial anastomosis tube  
1037 fusion during colony initiation in *Neurospora crassa*. *Fungal Genet Biol*  
1038 49:896-902.

1039 68. Bi Q, Wu D, Zhu X, & Gillian Turgeon B (2013) *Cochliobolus heterostrophus*  
1040 Llm1 - a Lae1-like methyltransferase regulates T-toxin production, virulence,  
1041 and development. *Fungal Genet Biol* 51:21-33.  
1042 69. Palmer JM, et al. (2013) Secondary metabolism and development is mediated  
1043 by LlmF control of VeA subcellular localization in *Aspergillus nidulans*. *PLoS*  
1044 *Genet* 9:e1003193.  
1045 70. Lombard V, Golaconda Ramulu H, Drula E, Coutinho PM, & Henrissat B (2014)  
1046 The carbohydrate-active enzymes database (CAZy) in 2013. *Nucleic Acids*  
1047 *Res* 42:D490-495.  
1048 71. Kim D, et al. (2013) TopHat2: accurate alignment of transcriptomes in the  
1049 presence of insertions, deletions and gene fusions. *Genome Biol* 14:R36.  
1050 72. Trapnell C, et al. (2013) Differential analysis of gene regulation at transcript  
1051 resolution with RNA-seq. *Nat Biotechnol* 31:46-53.  
1052 73. Ruepp A, et al. (2004) The FunCat, a functional annotation scheme for  
1053 systematic classification of proteins from whole genomes. *Nucleic Acids Res*  
1054 32:5539-5545.  
1055 74. Zhang Y, et al. (2008) Model-based analysis of ChIP-Seq (MACS). *Genome Biol*  
1056 9:R137.  
1057 75. Shannon P, et al. (2003) Cytoscape: a software environment for integrated  
1058 models of biomolecular interaction networks. *Genome Res* 13:2498-2504.  
1059 76. Krzywinski M, et al. (2009) Circos: an information aesthetic for comparative  
1060 genomics. *Genome Res* 19:1639-1645.  
1061  
1062

1063  
1064  
1065  
1066  
1067  
1068  
1069  
1070  
1071  
1072  
1073  
1074  
1075  
1076  
1077  
1078  
1079  
1080  
1081  
1082  
1083  
1084  
1085  
1086  
1087  
1088  
1089  
1090  
1091  
1092  
1093  
1094  
1095  
1096  
1097  
1098  
1099  
1100  
1101  
1102  
1103

Supplementary Information for

**The regulatory and transcriptional landscape associated with carbon utilization in a filamentous fungus**

Vincent W. Wu<sup>a,b</sup>, Nils Thieme<sup>c,g</sup>, Lori B. Huberman<sup>a,b</sup>, Axel Dietschmann<sup>c,f</sup>, Elias Bleek<sup>c</sup>, David J. Kowbel<sup>a</sup>, Juna Lee<sup>d</sup>, Sara Calhoun<sup>d</sup>, Vasanth Singan<sup>d</sup>, Anna Lipzen<sup>d</sup>, Yi Xiong<sup>a,b,h</sup>, Remo Monti<sup>d</sup>, Matthew J. Blow<sup>d</sup>, Ronan C. O'Malley<sup>d</sup>, Igor V. Grigoriev<sup>d,5</sup>, J. Philipp Benz<sup>d</sup>, N. Louise Glass<sup>a,b,e,1</sup>

<sup>a</sup>Department of Plant and Microbial Biology, University of California, Berkeley,  
<sup>b</sup>Energy Biosciences Institute, University of California, Berkeley,  
<sup>c</sup>Holzforschung München, TUM School of Life Sciences Weihenstephan, Technical University of Munich, Freising, Germany, <sup>d</sup>Joint Genome Institute, Walnut Creek, CA  
<sup>e</sup>Environmental Genomics and Systems Biology, Lawrence Berkeley National Laboratory, Berkeley, CA

<sup>1</sup>Corresponding Author: N. Louise Glass  
[Lglass@berkeley.edu](mailto:Lglass@berkeley.edu)

**This PDF file includes:**

Supplementary Materials and Methods  
Figures S1 to S5  
Tables S1, S2 and S5  
Legends for Table S3, Table S4 and Datasets S1 to S5  
SI References

**Other supplementary materials for this manuscript include the following:**

Table S3 and Table S4  
Datasets S1 to S5

**Materials and Methods**

**Strains, Growth Conditions and RNA extraction**

*N. crassa* wild type (FGSC 2489) and gene deletion strains (Table S5) were obtained from the Fungal Genetics Stock Center (1)(www.fgsc.net). The double deletion strains  $\Delta pdr-1$ ;  $\Delta pdr-2$  and  $\Delta vib-1$ ;  $\Delta clr-3$  were created by crossing the respective single deletion strains, selection with hygromycin B (Invitrogen), and

1104 confirmation by PCR. The  $\Delta$ NCU02853 and  $\Delta$ NCU08807 deletion strains were  
1105 generated as in (2) For Fig. S6b, a ;  $\Delta$ cre-1 delete from (3) was used. The *ara-1*  
1106 over-expression strain (OxNCU05414) was constructed by insertion of the *ara-1* ORF  
1107 into a vector having a glyceraldehyde-3-phosphate dehydrogenase (GPD) promoter  
1108 and a cyclosporin resistance marker (4), which was introduced into a  $\Delta$ *ara-1* strain.

1109 For all RNAseq experiments, conidia obtained from 10-day-old pre-grown  
1110 cultures were used to inoculate 3 ml of 1 x Vogel's salts (VMM) (5) plus 2% (w/v)  
1111 sucrose at  $1 \times 10^6$  cells/mL in 24 well Whatman Uniplates. The bottoms of the wells  
1112 for each Uniplate were initially scratched with a sharp needle to allow adherence  
1113 and formation of mycelial mat. After 16 hrs of growth, mycelia were washed three  
1114 times in 1 x VMM (5) without added carbon and subsequently transferred to 1 x  
1115 VMM with a new carbon source. For induction conditions, 2mM mono and  
1116 disaccharides were used, based on previously published reports for induction (6),  
1117 while for complex polysaccharides and plant biomass 1% (w/v) was used. Plant  
1118 biomass was obtained by grinding plant material to  $\sim .08$ mm size. Carbon  
1119 conditions and sources are included in Table S1. After 4 hrs of induction, mycelia  
1120 were harvested over Whatman #1 filter paper and flash frozen in liquid nitrogen for  
1121 storage at  $-80^\circ\text{C}$ . ~~Total RNA was isolated with TRIzol reagent (Invitrogen), treated~~  
1122 ~~with TURBO DNase (Thermo Fisher), and purified using Qiagen RNeasy Purification~~  
1123 ~~Kit. RNA was tested for quality using agarose gel electrophoresis. Three biological~~  
1124 ~~replicates were obtained and analyzed for every condition and strain.~~

1125 RNA extractions were performed on  $-80^\circ\text{C}$  stored biomass using TRIzol  
1126 (Invitrogen) and chloroform. Entire biomass sample from each 3ml cultures were  
1127 added to 1ml of TRIzol in a screwcap tube along with  $\sim .5\text{cm}^2$  of 0.1mm silica beads.  
1128 Tubes containing biomass, TRIzol and beads were bead beaten for 30 seconds, then  
1129 allowed to incubate at room temperature for 5 minutes on a rocker. 200ul of  
1130 chloroform was added to each tube, vortexed, and centrifuged for phase separation.  
1131 400ul of aqueous phase from each sample was combined with 400ul isopropanol  
1132 and incubated at room temperature for 10 minutes on rocker for RNA precipitation.  
1133 Samples were centrifuged at  $4^\circ\text{C}$  for 10 minutes. RNA pellets that formed were  
1134 washed with 75% ethanol and centrifuged at  $4^\circ\text{C}$  for 2 minutes. Ethanol was  
1135 removed via pipet, and RNA pellet allowed to dry for several minutes with cap open.  
1136 RNA pellet was resuspended in 40ul water, and treated with 2ul of Turbo DNase  
1137 (Thermo Fisher), in a 50ul reaction. After 20 minute incubation at  $37^\circ\text{C}$ , RNA was  
1138 cleaned up using Qiagen RNeasy Pufirication Kit. RNA was tested for quality using  
1139 agarose gel electrophoresis. Three biological replicates were obtained and analyzed  
1140 for every condition and strain.

#### 1141 1142 **RNA-seq**

1143 Stranded cDNA libraries were generated using the Illumina Truseq Stranded  
1144 RNA LT kit. mRNA was purified from 1  $\mu\text{g}$  of total RNA using magnetic beads  
1145 containing poly-dT oligos. mRNA was fragmented and reverse transcribed using  
1146 random hexamers and SSII (Invitrogen) followed by second strand synthesis. The  
1147 fragmented cDNA was treated with end-pair, A-tailing, adapter ligation, and  
1148 10 cycles of PCR. The prepared library was then quantified using KAPA Biosystem's  
1149 next-generation sequencing library qPCR kit and run on a Roche LightCycler 480  
1150 real-time PCR instrument. The quantified library was then multiplexed with other  
1151 libraries, and the pool of libraries was then prepared for sequencing on the Illumina  
1152 HiSeq sequencing platform utilizing a TruSeq paired-end cluster kit, v3, and  
1153 Illumina's cBot instrument to generate a clustered flowcell for sequencing.



1154 Sequencing of the flowcell was performed on the Illumina HiSeq2000 sequencer  
1155 using a TruSeq SBS sequencing kit, v3, following a 2x100 indexed run recipe.  
1156 Filtered reads were mapped against *N. crassa* OR74A genome (v12) using  
1157 Tophat 2.0.4 (7). Transcript abundance was estimated with Cufflinks 2.0.2 (8) in  
1158 fragments per kilobase of transcript per million mapped reads (FPKMs) using upper  
1159 quartile normalization and mapping against reference isoforms from the Broad  
1160 Institute. Tophat mapped reads were additionally counted by HTSeq 0.6.0 (9) to  
1161 obtain raw counts. Differential expression analysis was performed on raw counts  
1162 with DEseq2 version 3.3 (10) using data from biological triplicates. Hierarchical  
1163 clustering was performed using Python visualization library Seaborn  
1164 (<https://seaborn.pydata.org/>). Parameters for clustering of PCWDE expression  
1165 across 2mM sugar conditions: method = complete, metric = jaccard. Parameters  
1166 for clustering DEseq fold change for VIB-1 direct targets: method = weighted.  
1167 'Hierarchical Clustering Explorer' v3.5 software ([http://www.cs.umd.edu/hcil/multi-](http://www.cs.umd.edu/hcil/multi-cluster/hce3.html)  
1168 [cluster/hce3.html](http://www.cs.umd.edu/hcil/multi-cluster/hce3.html)) was used to compare the mean FPKMs of the RNA-Seq libraries  
1169 replicates (11, 12). A fold-change of  $2^{1.5}$  (corresponding to 2.8 -fold change) was  
1170 used because this cutoff used for these experiments included genes identified from  
1171 previous RNA-seq experiments that were direct targets of CLR-2 and XLR-1 (13).  
1172 Data is available here:  
1173 <https://genome.jgi.doe.gov/portal/TheFunENCproject/TheFunENCproject.info.html>  
1174

### 1175 **Weighted Correlation Network Analysis (WGCNA) and FUNCAT analyses**

1176 After filtering genes out due to low expression (<10 FKPM) across >95% of all  
1177 conditions, 6,742 genes were used in correlation analysis. The correlations were  
1178 scaled using soft power of 9, assuming a scale-free network. Hierarchical clustering  
1179 was applied to identify co-expressed gene modules with a minimum module size of  
1180 30 genes. The network with a force-directed layout was visualized using Cytoscape  
1181 version 3.3 (Shannon et al., 2003). The scaled correlations between gene pairs  
1182 above 0.15 are represented as edges in the network. Functional enrichment for the  
1183 gene modules was performed using functional assignments in FunCatDB (14). The  
1184 enrichment was calculated by the hypergeometric test and adjusted for multiple  
1185 hypothesis testing using the Bonferroni correction. CAZy gene annotations were  
1186 obtained from the JGI MycoCosm portal, Neucr2 (15).

1187

### 1188 **MFS transporter tree construction**

1189 Putative transporters were predicted using data from the transporter  
1190 classification database (TCDB) (<http://www.tcb.org/>) to generate a list of all *N.*  
1191 *crassa* transporters and major facilitator superfamily (MFS) transporters were  
1192 selected from this list. Protein sequences of all MFS genes were aligned using  
1193 MAFFT version 7 (16) and used to construct a maximum likelihood phylogeny using  
1194 RAxML (17). FigTree v1.4.2 (<http://tree.bio.ed.ac.uk/software/figtree/>) was used for  
1195 visualization.

### 1196 **Enzyme activity and transport assays**

1197 Strains were grown for 10 days in slants containing VMM (5) before conidia  
1198 were harvested.  $1 \times 10^6$  conidia/ml were transferred to 24 deep well plates  
1199 containing 3 ml of 1x VMM plus the appropriate carbon source. Uptake assays were  
1200 performed as described in (3, 18) with the following modifications. *N. crassa* WT,  
1201  $\Delta sut-28$ , and  $\Delta cre-1$  strains were pre-grown for 16 hr in 3 ml medium containing 1x  
1202 VMM and 2% sucrose. The mycelial biomass was washed three times in 1x VMM  
1203 solution and then transferred to an induction medium containing 1x VMM plus either



1204 0.5% pectin, 0.5% pectin and 2% (w/v) D-glucose (D-glc), or 0.5% xylan. The  
1205 samples were incubated for an additional 4 hrs and then washed again, as  
1206 described above. WT and  $\Delta cre-1$  strains were induced in 0.5% pectin or 0.5% pectin  
1207 plus 2% D-glc and transferred to either 100  $\mu$ M L-rha or 100  $\mu$ M L-rha plus 100  $\mu$ M D-  
1208 glc as uptake solution. WT and  $\Delta sut-28$  strains were transferred to uptake solutions  
1209 containing either 100  $\mu$ M L-rha, 90  $\mu$ M D-fucose (D-fuc, VWR, A16789), 90  $\mu$ M D-xyl  
1210 or 90  $\mu$ M D-galactose (D-gal, Sigma Aldrich, G0750).

1211 Cellulase activity assays were modified from Coradetti *et al* (19). Briefly, 3 x  
1212  $10^6$  conidia of the indicated strains were inoculated into 3 ml VMM + 2% sucrose in  
1213 round-bottomed, deep-well 24-well plates and grown at 25°C in constant light with  
1214 constant shaking at 200 rpm for 24 hr. The VMM + sucrose was vacuumed out of  
1215 the well and the mycelial cell mass was washed in VMM lacking a carbon source,  
1216 resuspended in media containing 2% Avicel as the sole carbon source, and  
1217 incubated as described above. Culture supernatants were harvested 72 hrs post-  
1218 transfer. Enzyme activity present in the culture supernatant was assayed with the  
1219 Remazol brilliant Blue R-conjugated carboxymethyl cellulose kit (Megazyme).

1220

### 1221 **Quantitative real-time PCR**

1222 Gene expression was analyzed by quantitative real-time PCR (RT-qPCR) as  
1223 described in (12). The expression of *sut-28* was determined for the WT and  $\Delta cre-1$   
1224 strains induced for 4 h on 1x VMM plus either 2 mM L-rha or 2 mM L-rhamnose  
1225 together with 2% D-glc. Relative expression levels were calculated against the WT  
1226 strain induced on 2 mM L-rhamnose. NCU09034 expression was analyzed for WT,  
1227  $\Delta pdr-1$ , and  $\Delta sut-28$  strains induced for 4 h on 1x VMM plus 2 mM L-rhamnose. The  
1228 actin gene (NCU04173) was used to normalize expression data.

1229

### 1230 **Genomic DNA library prep for DAP-seq**

1231 For genomic DNA isolation, the FGSC 2489 strain was grown on liquid VMM  
1232 for 24 hours at 25°C. Mycelia was filtered using Whatman #1 filter papers, and  
1233 collected into 2ml tubes for flash freezing in liquid N<sub>2</sub> and cell rupturing. Cell  
1234 rupturing was conducted by adding 1mm silica beads and along with DNA lysis  
1235 buffer (0.05M NaOH, 1mM EDTA, 1% TritonX) and placed into bead beater for 1  
1236 minute. DNA was purified using DNeasy Blood & Tissue kit (Qiagen Inc.). DNA was  
1237 sheared to 300 bp peak using Covaris LE220 sonicator. Size selection for sheared  
1238 DNA was performed using AMPure XP beads to remove DNA above and below target  
1239 molecular weight. Initially, sheared DNA was mixed in with AMPure XP beads (in  
1240 PEG-8000) at a ratio of 100:60. At this ratio, beads bind DNA with molecular weight  
1241 above 700 bp. Supernatant from this primary binding was taken and added to new  
1242 beads where final ratio of DNA solution to PEG-8000 was at 100:90. At this ratio,  
1243 DNA below ~300 bp does not bind to AMPure XP beads, and remaining DNA can be  
1244 eluted for library preparation. The KAPA library kit for Illumina sequencing was used  
1245 to prepare final libraries and stored at -20°C for later use.

1246

### 1247 **Transcription, translation, and DNA affinity purification (DAP)**

1248 Completed *in vitro* transcription and translation TnT reactions were incubated  
1249 with 20ng of genomic DNA libraries, 1ug salmon sperm for blocking and 20ul  
1250 Promega Magne HaloTag Beads on a rotator for 1 hr at room temperature. Bead  
1251 bound proteins along with protein bound DNA were washed three times with 2.5%  
1252 Tween20 in PBS. HaloTag beads were resuspended in 30ul ddH<sub>2</sub>O and heated to  
1253 98°C for 10 minutes to denature protein and release DNA fragments into solution.

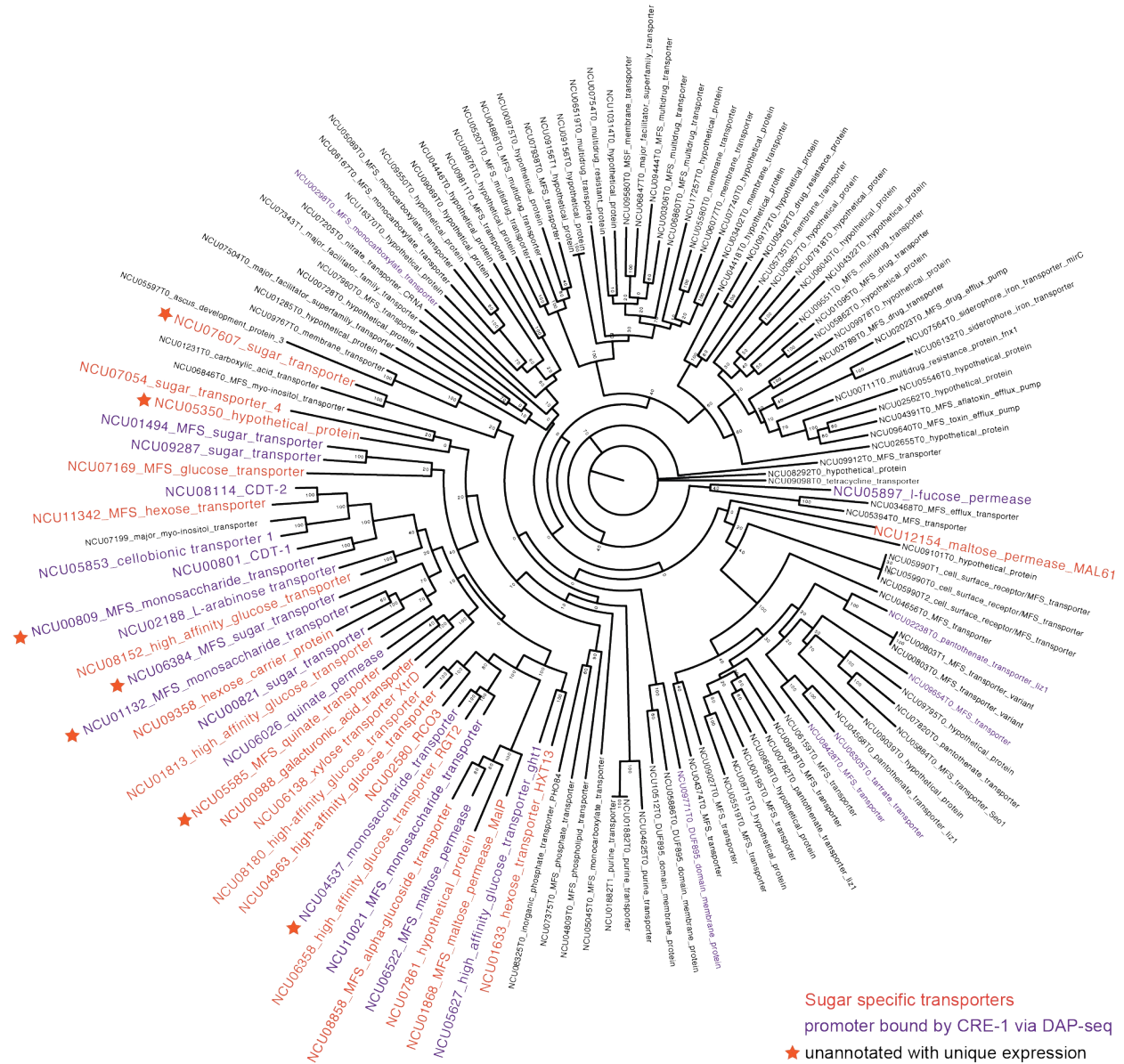
1254 Supernatant was transferred to a new tube for PCR amplification. DNA was amplified  
1255 for final libraries using KAPA Hifi polymerase for 12-16 cycles of PCR to generate  
1256 DAP-seq DNA libraries. A final DAP-seq DNA library was generated in the same  
1257 conditions with no added plasmid into TnT Master Mix as a negative control. Single  
1258 DAP-seq libraries were generated once for each transcription factor and sequenced  
1259 with Illumina MiSeq 2x150BP runs.

1260

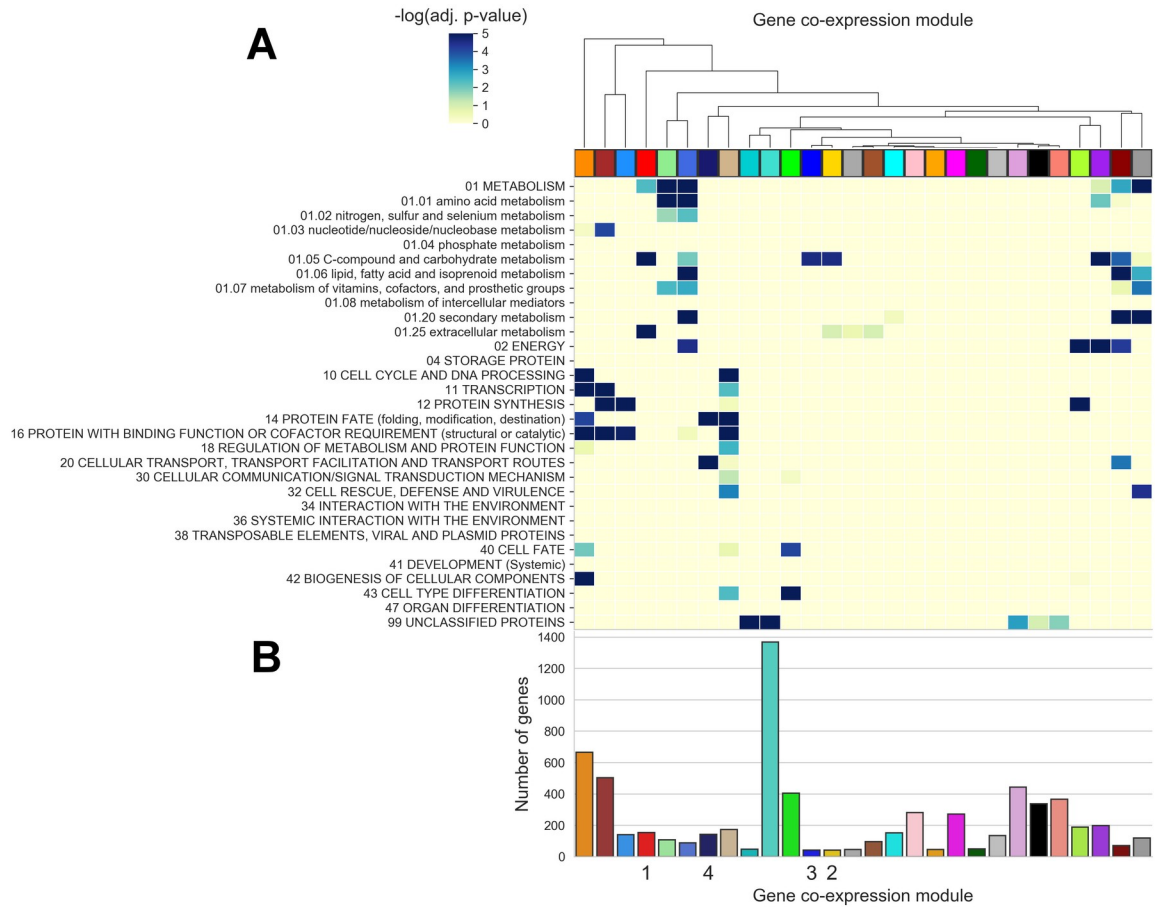
### 1261 **Motif construction**

1262 Motif discovery was performed using MEME v4.12.0 (20). Sequences of DAP-  
1263 seq binding peaks were used as input for MEME motif discovery with flags maxw  
1264 =20, minsites = 5, nmotifs = 8, denoting max width of motif, minimum number of  
1265 sites for each motif and number of motifs to generate respectively. For CRE-1 motif  
1266 discovery, all DAP-seq peaks within 3 kbp upstream of any translated genes were  
1267 utilized as input sequences. For XLR-1, XLR<sup>A828V</sup>, CLR-2 motif discovery, only DAP-  
1268 seq peaks within 3 kbp upstream and from genes with  $> 2^{1.5}$  fold reduction in  
1269  $\Delta$ transcription factor RNA-seq data sets as compared to wild type were utilized for  
1270 motif discovery. For VIB-1, DAP-seq peaks were within 1.5 kbp upstream for genes  
1271 with  $>2^{1.5}$  reduction in expression as compared to wild type for motif discovery.

1272



1274  
1275 **Fig. S1. MFS (Major Facilitator Superfamily) transporter maximum**  
1276 **likelihood tree.** Maximum likelihood tree built with RaxML (17). Bootstrap values  
1277 denoted in the nodes of each branch. Tips are labeled with Gene ID and Broad v12  
1278 annotation (<https://fungidb.org/fungidb/>). Highlighted in red and purple are  
1279 predicted or characterized sugar transporters. Marked with a red star are five  
1280 transporters, which show increased expression across varied plant cell wall sugars  
1281 at 2mM (SI Dataset 1). Highlighted in purple are transporter genes whose promoters  
1282 are bound by CRE-1 via DAP-seq (SI Dataset 4).  
1283

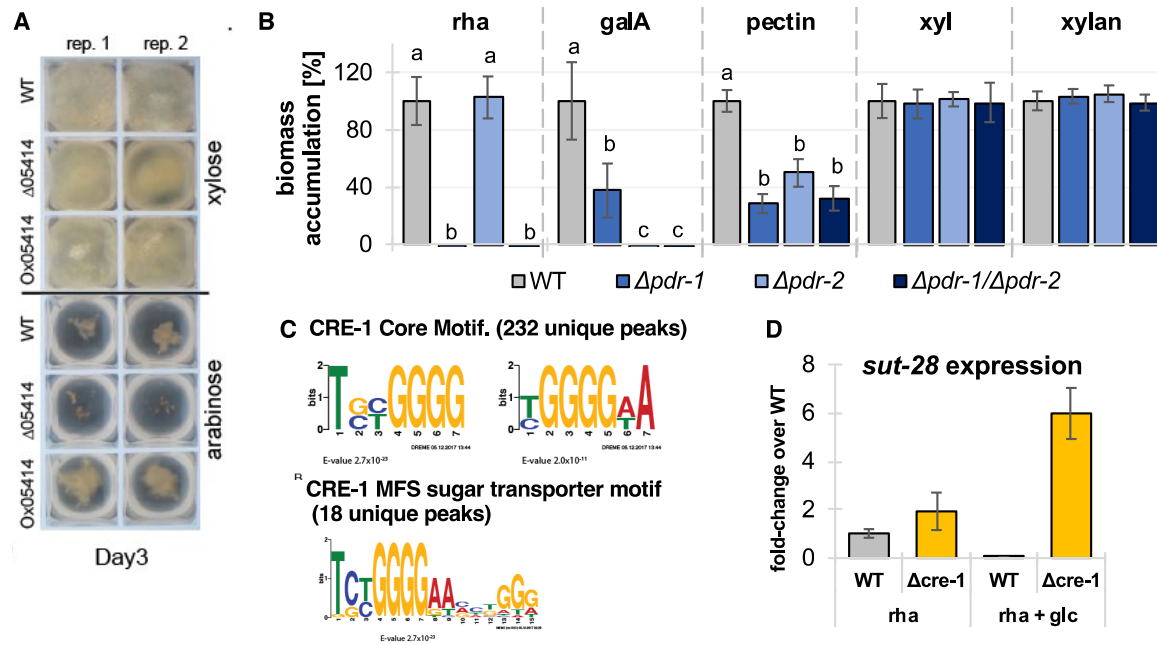


1284

1285

1286  
1287  
1288  
1289  
1290  
1291  
1292  
1293  
1294  
1295  
1296  
1297  
1298  
1299  
1300  
1301  
1302  
1303  
1304  
1305  
1306  
1307  
1308  
1309  
1310  
1311  
1312

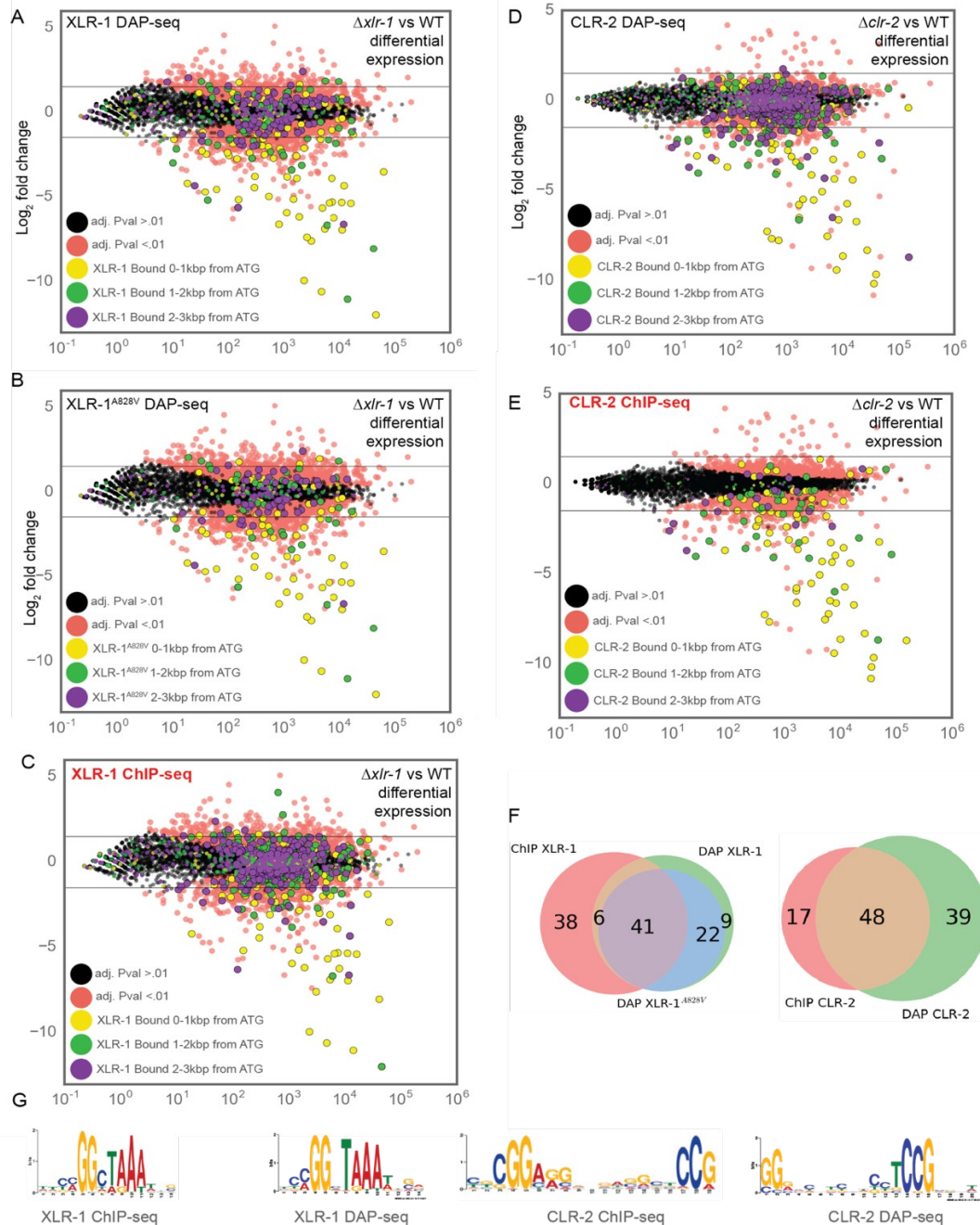
**Fig. S2. Weighted gene co-expression network analysis heatmap and module information.** (A) Heatmap of enrichment of general and metabolism-related functional categories by co-expressed gene module. Each column corresponds to a co-expressed gene module identified through weighted gene co-expression network analysis (WGCNA), with the same colors as the co-expressed gene modules shown in the network in Figure 1B. Each row corresponds to a functional category based on the classifications in FunCatDB (14). P-values reflect the significance of enrichment of genes assigned to a given functional category in a module and were calculated by the hypergeometric test. P-values were adjusted for multiple hypothesis testing using the Bonferroni correction. The color scale shows  $-\log_{10}$  p-value with the most significant groups shown in dark blue and least significant in yellow. The order of the columns was determined by hierarchical clustering of modules on the  $-\log_{10}$  p-values. (B) Number of genes in each co-expressed gene module from Figure 1B. See SI Dataset 2 for annotation of genes within the modules. ~~**Figure S2. Weighted gene co-expression network analysis heatmap and module information.** (A) Heatmap of enrichment of general and metabolism-related functional enrichment was performed using functional assignments in FunCatDB (14). Enrichment was calculated by the hypergeometric test and adjusted for multiple hypothesis testing using the Bonferroni correction. CAZyme gene annotations were obtained from the JGI MycoCosm portal, Neucr2 (15). The color scale shows  $-\log_{10}$  p-value with the most significant groups shown in dark blue and least significant in yellow. (B) Number of genes in each co-expressed gene module from Figure 1B. See SI Dataset 2 for annotation of genes within the modules.~~



1313  
1314  
1315  
1316  
1317  
1318  
1319  
1320  
1321  
1322  
1323  
1324  
1325  
1326  
1327  
1328  
1329

**Figure S3. Growth of  $\Delta pdr$  mutants and *ara-1* over-expression strain on different carbon sources, CRE-1 binding motifs and *sut-28* expression in a  $\Delta cre-1$  mutant.** (A) Biomass accumulation after shift to xylose or arabinose in WT,  $\Delta ara-1$  ( $\Delta 05415$ ) and *ara-1* over-expression (Ox0514) strains. (B) Relative biomass of FGSC2489 and  $\Delta sut-28$  strain incubated in rhamnose, polygalacturonic acid, pectin, xylose, and xylan as determined by dry weight. (n=3) Significance was determined by ANOVA followed by a post-hoc Tukey's test. Different letters above bars represent significant difference ( $p < 0.05$ ). (C) Top panel: Two CRE-1 binding motifs built using DREME v4.12.0 using all 232 DAP-seq peaks with the lowest E-value. Bottom panel: CRE-1 binding motifs built using MEME v4.12.0 using 18 DAP-seq binding peaks within the promoters of sugar transporters. (D) Relative expression of *sut-28* relative to *act* in FGSC2489 and  $\Delta cre-1$  mutants. Strains were either induced in rhamnose or on rhamnose plus glucose (n >=3)



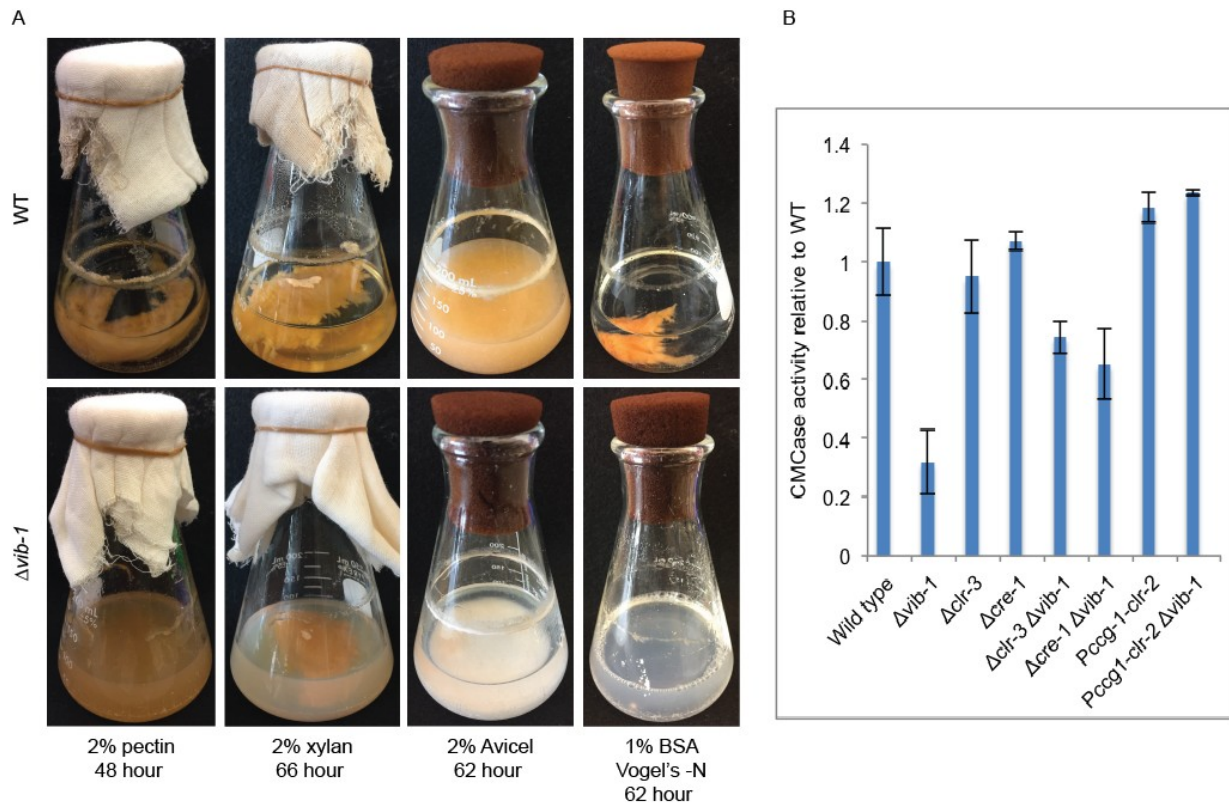


1330  
1331  
1332  
1333  
1334  
1335  
1336  
1337  
1338  
1339  
1340  
1341

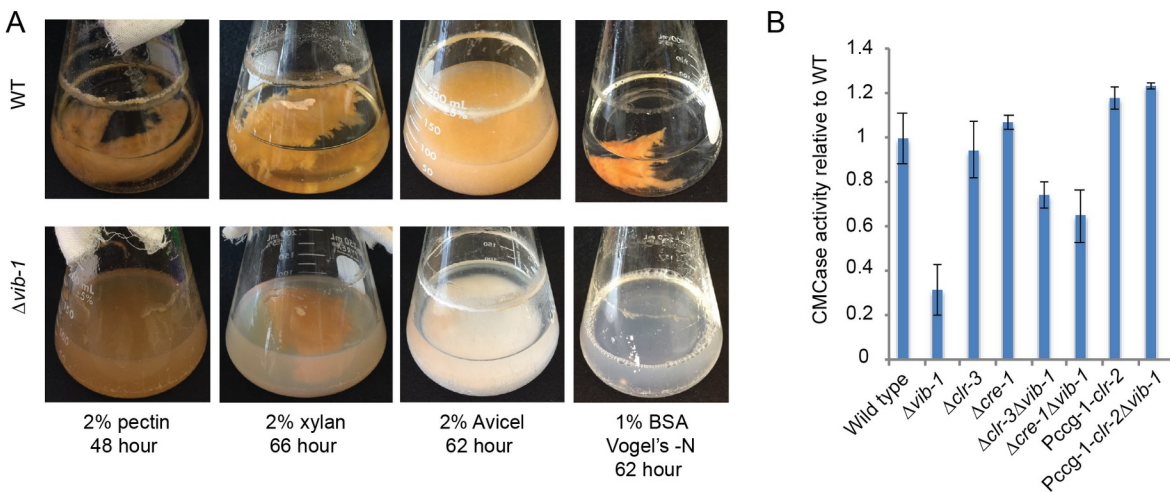
**Fig. S4. DAP-seq validation utilizing published CHIP-seq data of XLR-1 and CLR-2.** (A-E) Genes with XLR-1 DAP-seq, XLR-1<sup>A828V</sup> DAP-seq, XLR-1 ChIP-seq CLR-2 DAP-seq, and CLR2 ChIP-seq peaks overlaid onto differential expression data scatterplots of WT vs  $\Delta xlr-1$  shifted to 1% xylan or WT vs  $\Delta clr-2$  shifted to 1% Avicel, respectively. Gray lines represent chosen biological significance cutoff of  $\pm 2^{1.5}$ -fold change. Genes whose promoters are bound according to DAP-seq are highlighted in yellow, green or purple based on their distance from the ATG translation start site. “Base mean” is the mean of normalized counts for triplicates of both conditions tested. (F) Venn diagrams of direct targets from CHIP-seq (13) versus XLR-1 DAP-seq versus XLR-1<sup>A828V</sup> DAP-seq and Venn diagram of CLR-2 direct targets as

1342 discovered by ChIP-seq (13) versus DAP-seq. (G) XLR-1 and CLR-2 binding motifs  
1343 built from binding peaks from differentially expressed genes whose promoters have  
1344 binding peak sequences as discovered by ChIP-seq (13) versus DAP-seq. Motifs  
1345 | were built using DREME v4.12.0.  
1346 |

1347



1348



1349

1350

1351

1352

1353

1354

1355

1356

1357

1358

**Fig. S5.  $\Delta vib-1$  growth phenotypes on different carbon sources.**

(A)  $\Delta vib-1$  shows reduced growth and substrate depolymerization with pectin, xylan, or Avicel as the sole carbon source or BSA (as the sole carbon and nitrogen source). Cultures were directly inoculated from conidia at 25°C at 200rpm, and pictures taken at the time at which WT cultures were able to depolymerize and clear the substrate. (B) CMCase activity of enzymes secreted into culture supernatants by the indicated strains relative to wild type 72h post-shift to media containing Avicel as the sole carbon source (p-adj<0.01, Student's *t*-test with Benjamini/Hochberg multiple hypothesis correction). *Pccg-1-clr-2* strains have constitutive expression of

1359 *clr-2*, which results in inducer-independent induction of the CLR-2 cellulose regulon  
1360 (21). ( $n \geq 3$ )  
1361  
1362  
1363

1364 **Table S1: Carbon sources used in this study**

1365

1366

1367

Condition	Source	CAS Number
sucrose	Sigma	57-50-1
fructose	Research organics	0609-06-03
xylose	Acros Organics 225990050	58-86-6
mannose	Acros D (+) 99+%	3458-38-4
maltose	Sigma D (+) min 98% <0.3% glucose <1.0% maltotriose	6363-53-7
arabinose	Sigma L (+) min 99% a3256	5328-37-0
cellobiose	Fluka D (+) >99%	
galactose	Acros D (+) 99+%	59-23-4
rhamnose	TCI R0013	10030-85-0
galacturonic acid	fluka 48280	
glucuronic acid	Sigma 98%	12/3/56
trehalose	Acros D 99%	6138-23-4
mannobiose	Megazyme	O-MBI
sorbose	Calbiochem L(-) 99.6%	CAS 87-79-6
glycerol	Fisher	56-81-5
ribose	TCI R0025	50-69-1
mannitol	Fisher	69-65-8
fucose	Sigma	<u>2438-80-4</u>
inulin	Sigma	9005-80-5
Avicel	Fluka	9004-34-6
xylan	Sigma from beechwood	9014-63-5
xyloglucan	Megazyme (from tamarind)	
galactomannan	Megazyme (carob low viscosity)	
glucomannan	Konjac Foods	
mixed linkage glucan	Megazyme (barley)	
pectin	Sigma from orange peel	<u>9000-69-5</u>
pectin esterified	Sigma	<u>9046-40-6</u>
polygalacturonic acid	Sigma	<u>25990-10-7</u>
rhamnogalacturon an	Megazyme (potato)	
arabinan	Megazyme (sugar beet)	
galactan	Megazyme (lupin)	
amylopectin	Sigma from corn A-7780	
amylose	Sigma from corn A-7043	
dioxane lignin	in house	
citrus peel	in house	
Miscanthus	in house	
corn stover	in house	
Wing Nut	in house	
Energy Cane	in house	
Switchgrass	in house	

1368 **Table S2. Predicted genes in the *Neurospora crassa* genome encoding**  
 1369 **plant biomass degrading enzymes and sugar transporters**

Gene ID	Annotation	Gene name/enzyme family/TCBD <sup>1</sup>
NCU08412	beta-1,4-endomannanase	<i>gh5-7</i>
NCU00985	extracellular beta-mannosidase	<i>gh2-4</i>
NCU00890	intracellular beta-mannosidase	<i>gh2-1</i>
NCU08131	alpha-amylase	GH13
NCU09805	alpha-amylase	GH13
NCU05873	alpha-amylase	GH13
NCU05429	alpha-amylase	GH13
NCU06523	intracellular alpha-glucosidase	<i>gh13-4</i>
NCU07860	intracellular alpha-glucosidase	<i>gh13-5</i>
NCU03098	intracellular alpha-glucosidase	<i>gh15-1</i>
NCU00743	amylo-alpha-1,6-glucosidase	<i>gh13-7</i>
NCU01517	extracellular alpha-glucosidase <i>gla-1</i>	GH15
NCU02583	extracellular alpha-glucosidase	GH31
NCU09281	extracellular alpha-glucosidase	<i>gh31-1</i>
NCU04203	extracellular alpha-glucosidase	<i>gh31-2</i>
NCU04674	extracellular alpha-glucosidase	<i>gh31-3</i>
NCU04221	neutral trehalase	GH37
NCU08746	starch active LPMO	AA13
NCU00943	trehalase	GH37
NCU09170	alpha-arabinofuranosidase	<i>gh43-4</i>
NCU05965	alpha-arabinofuranosidase	<i>gh43-7</i>
NCU02343	alpha-arabinofuranosidase	<i>gh51-1</i>
NCU09775	alpha-arabinofuranosidase	<i>gh54-1</i>
NCU00642	extracellular beta-galactosidase	<i>gh35-1</i>
NCU04623	extracellular beta-galactosidase	<i>gh35-2</i>
NCU06861	glycosyl hydrolase family 43 protein	GH43
NCU01900	intracellular beta-xylosidase	<i>gh43-2</i>
NCU00972	endo-beta-1,4-galactanase	<i>gh53-1</i>
NCU05882	endo-beta-1,6-galactanase	<i>gh5-5</i>
NCU09702	endo-beta-1,6-galactanase	<i>gh5-6</i>
NCU00852	endoarabinanase	<i>gh43-1</i>
NCU02369	endogalacturonase	<i>gh28-1</i>
NCU06961	exogalacturonase	GH28
NCU09924	exoarabinanase	GH93
NCU00937	extracellular beta-glucuronidase	<i>gh79-1</i>
NCU09774	feruloyl esterase C	CE1
NCU09491	feruloyl esterase B <i>fae-1</i>	CE1
NCU08785	feruloyl esterase D <i>faeD</i>	CE1
NCU06326	pectate lyase <i>ply-1</i>	GH76
NCU08176	pectate lyase <i>ply-2</i>	PL3

NCU10045	pectin methyl esterase	<i>ce8-1</i>
NCU09976	rhamnogalacturonan acetyl esterase	<i>ce12-1</i>
NCU05598	rhamnogalacturonan lyase <i>asd-1</i>	PL4
NCU02654	unsaturated rhamnogalacturonyl hydrolase	<i>gh105-1</i>
NCU07351	alpha-glucuronidase	GH67
NCU06143	alpha-glucuronidase	GH67
NCU04885	alpha-xylosidase	GH31
NCU05924	beta-1,4-endoxylanase	<i>gh10-1</i>
NCU08189	beta-1,4-endoxylanase	<i>gh10-2</i>
NCU04997	beta-1,4-endoxylanase	<i>gh10-3</i>
NCU07130	beta-1,4-endoxylanase	<i>gh10-4</i>
NCU02855	beta-1,4-endoxylanase	<i>gh11-1</i>
NCU07225	beta-1,4-endoxylanase	<i>gh11-2</i>
NCU09923	extracellular beta-xylosidase	<i>gh3-7</i>
NCU00709	extracellular beta-xylosidase	<i>gh3-8</i>
NCU04870	acetyl xylan esterase	CE1
NCU04494	acetyl xylan esterase	CE1
NCU00710	acetyl xylan esterase	CE1
NCU05159	acetyl xylan esterase	CE1
NCU09663	acetyl xylan esterase	CE1
NCU09664	acetyl xylan esterase	CE1
NCU03181	acetyl xylan esterase	CE1
NCU00762	beta-1,4-endoglucanase	<i>gh5-1</i>
NCU05057	beta-1,4-endoglucanase	<i>gh7-1</i>
NCU04854	beta-1,4-endoglucanase	<i>gh7-2</i>
NCU04027	beta-1,4-endoglucanase	<i>gh7-3</i>
NCU05121	beta-1,4-endoglucanase	<i>gh45-1</i>
NCU05955	beta-1,4-endoglucanase	<i>gh74-1</i>
NCU00206	cellobiose dehydrogenase	CDH
NCU05923	cellobiose dehydrogenase	CDH
NCU03996	exo-beta-1,4-glucanase or cellobiohydrolase	<i>gh6-1</i>
NCU09680	exo-beta-1,4-glucanase or cellobiohydrolase	<i>gh6-2</i>
NCU07190	exo-beta-1,4-glucanase or cellobiohydrolase	<i>gh6-3</i>
NCU07340	cellobiohydrolase <i>cbh-1</i>	GH7
NCU05104	exo-beta-1,4-glucanase or cellobiohydrolase	<i>gh7-4</i>
NCU08760	polysaccharide monooxygenase 1 (PMO1)	AA9
NCU03328	polysaccharide monooxygenase 1 (PMO1)	AA9
NCU00836	polysaccharide monooxygenase 1 (PMO1)	AA9
NCU01867	polysaccharide monooxygenase 1 (PMO1)	AA9
NCU02344	polysaccharide monooxygenase 1 (PMO1)	AA9
NCU09764	polysaccharide monooxygenase 1 (PMO1)	AA9
NCU02240	polysaccharide monooxygenase 2 (PMO2)	AA9
NCU02916	polysaccharide monooxygenase 2 (PMO2)	AA9
NCU01050	polysaccharide monooxygenase 2 (PMO2)	AA9



NCU07760	polysaccharide monooxygenase 3 (PMO3)	AA9
NCU03000	polysaccharide monooxygenase 3 (PMO3)	AA9
NCU05969	polysaccharide monooxygenase 3 (PMO3)	AA9
NCU07520	polysaccharide monooxygenase 3 (PMO3)	AA9
NCU07898	polysaccharide monooxygenase 3 (PMO3)	AA9
NCU07974	polysaccharide monooxygenase 3 (PMO3)	AA9
NCU03641	extracellular beta-glucosidase	GH3
NCU08755	extracellular beta-glucosidase	GH3
NCU04952	extracellular beta-glucosidase	GH3
NCU00130	intracellular beta-glucosidase	GH1
NCU08054	intracellular beta-glucosidase	GH3
NCU05577	intracellular beta-glucosidase	GH3
NCU07487	intracellular beta-glucosidase	GH3
NCU09533	galacturonic acid reductase (GaaA)	
NCU07064	L-galactonate-dehydratase (GaaB)	
NCU09532	L-threo-3-deoxy-hexulose-5-phosphate aldolase (GaaC)	
NCU01906	put. L-glyceraldehyde reductase (GaaD)	
NCU09035	L-rhamnose-1-dehydrogenase LRA1	
NCU03605	L-rhamnono- $\gamma$ -lactonase LRA2	
NCU09034	rhamnonate dehydratase LRA3	
NCU05037	L- and L-KDR aldolase LRA4	
NCU00643	L-arabinitol-dehydrogenase <i>ard-1</i>	
NCU02188	L-arabinose transporter <i>lat-1</i>	
NCU00891	xylitol dehydrogenase	
NCU08384	xylose/arabinose reductase	
NCU09041	xylulose reductase	
NCU08687	galactokinase	
NCU04460	galactose-1-phosphate uridylyltransferase	
NCU08549	UDP-galactose 4-epimerase	
NCU07607	sugar transporter	2.A.1.12.2
NCU00450	sucrose transporter	2.A.2.6.1
NCU00801	cellodextrone transporter <i>cdt-1</i>	2.A.1.1.9
NCU00809	MFS monosaccharide transporter	2.A.1.1.9
NCU00821	sugar transporter	2.A.1.1.73
NCU00988	galacturonic acid transporter <i>gat-1</i>	2.A.1.1.7
NCU01132	MFS monosaccharide transporter	2.A.1.1.38
NCU01231	carboxylic acid transporter	2.A.1.12.2
NCU01494	MFS sugar transporter	2.A.1.1.69
NCU01633	hexose transporter HXT13	2.A.1.1.58
NCU01813	high affinity glucose transporter	2.A.1.1.39
NCU01868	MFS maltose permease MalP	2.A.1.1.10
NCU02188	L-arabinose transporter <i>lat-1</i>	2.A.1.1.39

NCU02582	sorbose-resistant-4	2.A.1.1.51
NCU04537	monosaccharide transporter	2.A.1.1.57
NCU04963	high-affinity glucose transporter	2.A.1.1.51
NCU05350	MFS transporter	2.A.1.1.40
NCU05585	MFS quinate transporter	2.A.1.1.7
NCU05627	high affinity glucose transporter ght1	2.A.1.1.36
NCU05853	cellobionic acid transporter cbt-1	2.A.1.1.9
NCU05897	l-fucose permease (rhamnose transporter)	2.A.1.7.1
NCU06026	quinat permease	2.A.1.1.7
NCU06138	xylose transporter XtrD aspergillus	2.A.1.1.40
NCU06358	high affinity glucose transporter RGT2	2.A.1.1.57
NCU06384	MFS sugar transporter	2.A.1.1.38
NCU06522	MFS maltose permease	2.A.1.1.10
NCU07054	sugar transporter 4	2.A.1.1.57
NCU07169	MFS glucose transporter	2.A.1.1.43
NCU07199	major myo-inositol transporter ioIT	2.A.1.1.9
NCU07861	MFS transporter	2.A.1.1.10
NCU08114	cellodextrose transporter cdt-2	2.A.1.1.9
NCU08152	high affinity glucose transporter	2.A.1.1.39
NCU08180	high-affinity glucose transporter	2.A.1.1.68
NCU08858	MFS alpha-glucoside transporter	2.A.1.1.10
NCU09287	sugar transporter	2.A.1.1.69
NCU09321	sucrose transporter	2.A.2.6.1
NCU09358	hexose carrier protein	2.A.1.1.73
NCU10021	MFS monosaccharide transporter	2.A.1.1.57
NCU11342	MFS hexose transporter	2.A.1.1.9
NCU12154	maltose permease MAL61	2.A.1.1.11

1370 <sup>1</sup>**TCDB:** The Transporter Classification Database (22).

1371 **Table S3. Predicted genes encoding DNA binding proteins in the *N. crassa***  
1372 **genome and carbon conditions used for testing expression of 34**  
1373 **transcription factors mutants**  
1374  
1375  
1376 **Table S4. Functional category (FunCAT) analyses of CRE-1-bound genes**

1377 **Table S5. Strains used in this study**

<b>Name</b>	<b>Genotype</b>	<b>Source</b>
Wild type	<i>Wild type mat A</i>	FGSC 2489 (1)
$\Delta$ NCU08042 ( <i>clr-2</i> )	$\Delta$ <i>clr-2::hygR mat A</i>	FGSC 15834
$\Delta$ NCU07705 ( <i>clr-1</i> )	$\Delta$ <i>clr-1::hygR mat A</i>	FGSC 11028
$\Delta$ NCU06971 ( <i>xlr-1</i> )	$\Delta$ <i>xlr-1::hygR mat A</i>	FGSC 11067
$\Delta$ NCU05414 ( <i>ara-1</i> )	$\Delta$ NCU05414 ( <i>ara-1</i> ):: <i>hygR mat A</i>	FGSC 21219
$\Delta$ NCU04295 ( <i>pdr-2</i> )	$\Delta$ NCU04295 ( <i>pdr-2</i> ):: <i>hygR mat a</i>	FGSC 18855
$\Delta$ NCU09033 ( <i>pdr-1</i> )	$\Delta$ NCU09033 ( <i>pdr-1</i> ):: <i>hygR mat A</i>	FGSC 09033
$\Delta$ NCU03725 ( <i>vib-1</i> )	$\Delta$ NCU03725 ( <i>vib-1</i> ):: <i>hygR mat A</i>	FGSC 11309
$\Delta$ NCU00282	$\Delta$ NCU00282:: <i>hygR mat a</i>	FGSC 12566
$\Delta$ NCU00289	$\Delta$ NCU00289:: <i>hygR mat A</i>	FGSC 11086
$\Delta$ NCU00808	$\Delta$ NCU00808:: <i>hygR mat A</i>	FGSC 11123
$\Delta$ NCU10080	$\Delta$ NCU10080:: <i>hygR mat A</i>	FGSC 17448
$\Delta$ NCU01074	$\Delta$ NCU01074:: <i>hygR mat A</i>	FGSC 17482
$\Delta$ NCU01154 ( <i>sub-1</i> )	$\Delta$ NCU01154:: <i>hygR mat A</i>	FGSC 11126
$\Delta$ NCU01209	$\Delta$ NCU01209:: <i>hygR mat a</i>	FGSC 17008
$\Delta$ NCU01312 ( <i>rca-1</i> )	$\Delta$ NCU01312:: <i>hygR mat A</i>	FGSC 11209
$\Delta$ NCU01386	$\Delta$ NCU01386:: <i>hygR mat A</i>	FGSC 16372
$\Delta$ NCU01640 ( <i>rpn-4</i> )	$\Delta$ NCU01640:: <i>hygR mat A</i>	FGSC 11195
$\Delta$ NCU02203	$\Delta$ NCU02203:: <i>hygR mat A</i>	FGSC 11884
$\Delta$ NCU02307	$\Delta$ NCU02307:: <i>hygR mat a</i>	FGSC 11054
$\Delta$ NCU02853	$\Delta$ NCU02853:: <i>hygR mat A</i>	this study
$\Delta$ NCU03421	$\Delta$ NCU03421:: <i>hygR mat a</i>	FGSC 11149
$\Delta$ NCU03417	$\Delta$ NCU03417:: <i>hygR mat A</i>	FGSC 21249
$\Delta$ NCU03643	$\Delta$ NCU03643:: <i>hygR mat A</i>	FGSC 11049
$\Delta$ NCU03699	$\Delta$ NCU03699:: <i>hygR mat a</i>	FGSC 11130
$\Delta$ NCU04058	$\Delta$ NCU04058:: <i>hygR mat a</i>	FGSC 17238
$\Delta$ NCU04211	$\Delta$ NCU04211:: <i>hygR mat a</i>	FGSC 11133
$\Delta$ NCU04848	$\Delta$ NCU04848:: <i>hygR mat A</i>	FGSC 16718
$\Delta$ NCU04851	$\Delta$ NCU04851:: <i>hygR mat a</i>	FGSC 11089
$\Delta$ NCU05024	$\Delta$ NCU05024:: <i>hygR mat A</i>	FGSC 14730
$\Delta$ NCU05909	$\Delta$ NCU05909:: <i>hygR mat a</i>	FGSC 11104
$\Delta$ NCU06173	$\Delta$ NCU06173:: <i>hygR mat A</i>	FGSC 11366
$\Delta$ NCU06920	$\Delta$ NCU06920:: <i>hygR mat A</i>	FGSC 17870
$\Delta$ NCU07728 ( <i>sre-1</i> )	$\Delta$ NCU07728:: <i>hygR mat a</i>	FGSC 11268
$\Delta$ NCU08055	$\Delta$ NCU08055:: <i>hygR mat A</i>	FGSC 11269
$\Delta$ NCU08634	$\Delta$ NCU08634:: <i>hygR mat a</i>	FGSC 20296
$\Delta$ NCU08899	$\Delta$ NCU08899:: <i>hygR mat a</i>	FGSC 11048
$\Delta$ NCU09169	$\Delta$ NCU09169:: <i>hygR mat A</i>	FGSC 19656
$\Delta$ NCU09252	$\Delta$ NCU09252:: <i>hygR mat A</i>	FGSC 11394
$\Delta$ NCU10697	$\Delta$ NCU10697:: <i>hygR mat A</i>	FGSC 21637
$\Delta$ NCU05897	$\Delta$ NCU05897:: <i>hygR mat A</i>	FGSC 13717
$\Delta$ <i>pdr-1<math>\Delta</math><i>pdr-2</i></i>	$\Delta$ NCU09033:: <i>hygR</i> ; $\Delta$ NCU04295:: <i>hygR mat a</i>	this study
$\Delta$ <i>cre-1</i>	$\Delta$ <i>cre-1::hygR mat A</i>	this study
OxNCU05414 ( <i>ara-1</i> )	<i>pgpd-1</i> -NCU05414: <i>csr-1</i> ; $\Delta$ NCU05414:: <i>hygR mat A</i>	this study
SC4B5	$\Delta$ <i>clr-3::hyg<sup>R</sup> mat A</i>	FGSC 14350 (2)
SC1B3	$\Delta$ <i>vib-1::hyg<sup>R</sup> mat a</i>	FGSC 11308 (2)
LHN694	<i>P<sub>ccg-1</sub>-clr-2::his-3</i> $\Delta$ <i>sad-1::hyg<sup>R</sup> rid-</i>	(21)

	<i>1</i> ; $\Delta$ <i>clr-2::hyg<sup>R</sup></i> <i>mat A</i>	
LHN971	$\Delta$ <i>vib-1::hyg<sup>R</sup></i> ; $\Delta$ <i>clr-3::hyg<sup>R</sup></i> <i>mat a</i>	This study
LHN972	$\Delta$ <i>vib-1::hyg<sup>R</sup></i> ; $\Delta$ <i>clr-3::hyg<sup>R</sup></i> <i>mat A</i>	This study
LHN898	$\Delta$ <i>cre-1::hyg<sup>R</sup></i> <i>mat A</i>	(3)
VW205	$\Delta$ <i>cre-1::hyg<sup>R</sup></i> ; $\Delta$ <i>vib-1::hyg<sup>R</sup></i> <i>mat a</i>	(23)
VW206	<i>P<sub>ccg-1</sub>-clr-2::his-3</i> $\Delta$ <i>sad-1::hyg<sup>R</sup></i> <i>rid-1</i> ; $\Delta$ <i>clr-2::hyg<sup>R</sup></i> ; $\Delta$ <i>vib-1::hyg<sup>R</sup></i> <i>mat A</i>	(23)

1378  
1379

- 1380 **SI Dataset 1.** Normalized FPKM counts of wild type cells and selected  
1381 mutants exposed to carbon conditions (Table S1)
- 1382 **SI Dataset 2.** Lists of genes within 28 modules from WCGNA analysis
- 1383 **SI Dataset 3.** DE-seq analysis of expression profiles of  $\Delta clr-1$ ,  $\Delta clr-2$ ,  $\Delta xlr-1$ ,  
1384  $\Delta pdr-2$  (NCU04295),  $\Delta ara-1$  (NCU05414) and  $\Delta vib-1$  transcription factor  
1385 mutants on various carbon sources
- 1386 **SI Dataset 4.** DAP-seq data on XLR-1, XLR-1<sup>A828V</sup>, CLR-2, CRE-1, VIB-1, and  
1387 reanalyzed data for CHIP-seq data for XLR-1 and CLR-2
- 1388 **SI Dataset 5.** The VIB-1 direct targets and core VIB-1 regulon based on RNA-  
1389 seq and DAP-seq data  
1390

1391 | **References NOT UPDATED**

- 1392 1. McCluskey K (2003) The Fungal Genetics Stock Center: from molds to  
1393 molecules. *Adv. Appl. Microbiol.* 52:245-262.
- 1394 2. Colot HV, *et al.* (2006) A high-throughput gene knockout procedure for  
1395 *Neurospora* reveals functions for multiple transcription factors. *Proc Natl Acad*  
1396 *Sci U S A* 103:10352-10357.
- 1397 3. Huberman LB, Coradetti ST, & Glass NL (2017) Network of nutrient-sensing  
1398 pathways and a conserved kinase cascade integrate osmolarity and carbon  
1399 sensing in *Neurospora crassa*. *Proc Natl Acad Sci U S A* 114:E8665-E8674.
- 1400 4. Bardiya N & Shiu PK (2007) Cyclosporin A-resistance based gene placement  
1401 system for *Neurospora crassa*. *Fungal Genet Biol* 44:307-314.
- 1402 5. Vogel HJ (1956) A convenient growth medium for *Neurospora* (medium N).  
1403 *Microbial Genetics Bulletin* 13:42-43.
- 1404 6. Znameroski EA, *et al.* (2012) Induction of lignocellulose-degrading enzymes in  
1405 *Neurospora crassa* by cellodextrins. *Proc Natl Acad Sci USA* 109:6012-6017.
- 1406 7. Kim D, *et al.* (2013) TopHat2: accurate alignment of transcriptomes in the  
1407 presence of insertions, deletions and gene fusions. *Genome Biol* 14:R36.
- 1408 8. Trapnell C, *et al.* (2013) Differential analysis of gene regulation at transcript  
1409 resolution with RNA-seq. *Nat Biotechnol* 31:46-53.
- 1410 9. Anders S, Pyl PT, & Huber W (2015) HTSeq--a Python framework to work with  
1411 high-throughput sequencing data. *Bioinformatics* 31:166-169.
- 1412 10. Love MI, Huber W, & Anders S (2014) Moderated estimation of fold change  
1413 and dispersion for RNA-seq data with DESeq2. *Genome Biol* 15:550.
- 1414 11. Thieme N, *et al.* (2017) The transcription factor PDR-1 is a multi-functional  
1415 regulator and key component of pectin deconstruction and catabolism in  
1416 *Neurospora crassa*. *Biotechnol Biofuels* 10:149.
- 1417 12. Benz JP, *et al.* (2014) A comparative systems analysis of polysaccharide-  
1418 elicited responses in *Neurospora crassa* reveals carbon source-specific  
1419 cellular adaptations. *Mol Microbiol* 91:275-299.
- 1420 13. Craig JP, Coradetti ST, Starr TL, & Glass NL (2015) Direct target network of  
1421 the *Neurospora crassa* plant cell wall deconstruction regulators CLR-1, CLR-2,  
1422 and XLR-1. *MBio* 6(5).
- 1423 14. Ruepp A, *et al.* (2004) The FunCat, a functional annotation scheme for  
1424 systematic classification of proteins from whole genomes. *Nucleic Acids Res*  
1425 32:5539-5545.
- 1426 15. Grigoriev IV, *et al.* (2014) MycoCosm portal: gearing up for 1000 fungal  
1427 genomes. *Nucleic Acids Res* 42:D699-704.
- 1428 16. Katoh K, Misawa K, Kuma K, & Miyata T (2002) MAFFT: a novel method for  
1429 rapid multiple sequence alignment based on fast Fourier transform. *Nucleic*  
1430 *Acids Res* 30:3059-3066.
- 1431 17. Stamatakis A (2006) RAxML-VI-HPC: maximum likelihood-based phylogenetic  
1432 analyses with thousands of taxa and mixed models. *Bioinformatics* 22:2688-  
1433 2690.
- 1434 18. Ha SJ, *et al.* (2011) Engineered *Saccharomyces cerevisiae* capable of  
1435 simultaneous cellobiose and xylose fermentation. *Proc Natl Acad Sci USA*  
1436 108:504-509.
- 1437 19. Coradetti ST, *et al.* (2012) Conserved and essential transcription factors for  
1438 cellulase gene expression in ascomycete fungi. *Proc Natl Acad Sci USA*  
1439 109:7397-7402.



1440 20. Bailey TL, et al. (2009) MEME SUITE: tools for motif discovery and searching.  
1441 *Nucleic Acids Res* 37:W202-208.  
1442 21. Coradetti ST, Xiong Y, & Glass NL (2013) Analysis of a conserved cellulase  
1443 transcriptional regulator reveals inducer-independent production of  
1444 cellulolytic enzymes in *Neurospora crassa*. *Microbiologyopen* 2:595-609.  
1445 22. Saier MH, Jr., et al. (2016) The Transporter Classification Database (TCDB):  
1446 recent advances. *Nucleic Acids Res* 44:D372-379.  
1447 23. Xiong Y, Sun J, & Glass NL (2014) VIB1, a link between glucose signaling and  
1448 carbon catabolite repression, is essential for plant cell wall degradation in  
1449 *Neurospora crassa*. *PLoS Genet* 10:e1004500.  
1450  
1451  
1452

